JCI The Journal of Clinical Investigation

PAX7 expression defines germline stem cells in the adult testis

Gina M. Aloisio, … , F. Kent Hamra, Diego H. Castrillon

J Clin Invest. 2014;124(9):3929-3944. https://doi.org/10.1172/JCI75943.

Research Article

Spermatogenesis is a complex, multistep process that maintains male fertility and is sustained by rare germline stem cells. Spermatogenic progression begins with spermatogonia, populations of which express distinct markers. The identity of the spermatogonial stem cell population in the undisturbed testis is controversial due to a lack of reliable and specific markers. Here we identified the transcription factor PAX7 as a specific marker of a rare subpopulation of A_{single} spermatogonia in mice. $PAX7^+$ cells were present in the testis at birth. Compared with the adult testis, $PAX7^+$ cells constituted a much higher percentage of neonatal germ cells. Lineage tracing in healthy adult mice revealed that $PAX7^+$ spermatogonia self-maintained and produced expanding clones that gave rise to mature spermatozoa. Interestingly, in mice subjected to chemotherapy and radiotherapy, both of which damage the vast majority of germ cells and can result in sterility, $PAX7^+$ spermatogonia selectively survived, and their subsequent expansion contributed to the recovery of spermatogenesis. Finally, $PAX7^+$ spermatogonia were present in the testes of a diverse set of mammals. Our data indicate that the $PAX7^+$ subset of A_{single} spermatogonia functions as robust testis stem cells that maintain fertility in normal spermatogenesis in healthy mice and mediate recovery after severe germline injury, such as occurs after cancer therapy.

PAX7 expression defines germline stem cells in the adult testis

Gina M. Aloisio,[1] Yuji Nakada,[1] Hatice D. Saatcioglu,[1] Christopher G. Peña,[1] Michael D. Baker,[1] Edward D. Tarnawa,[2] Jishnu Mukherjee,[1] Hema Manjunath,[1] Abhijit Bugde,[3] Anita L. Sengupta,[1] James F. Amatruda,[4] Ileana Cuevas,[1] F. Kent Hamra,[5] and Diego H. Castrillon[1]

[1]Department of Pathology, [2]Department of Obstetrics and Gynecology, Division of Reproductive Endocrinology and Infertility, [3]Department of Cell Biology, [4]Departments of Internal Medicine, Molecular Biology, and Pediatrics, and [5]Department of Pharmacology, UT Southwestern Medical Center, Dallas, Texas, USA.

Spermatogenesis is a complex, multistep process that maintains male fertility and is sustained by rare germline stem cells. Spermatogenic progression begins with spermatogonia, populations of which express distinct markers. The identity of the spermatogonial stem cell population in the undisturbed testis is controversial due to a lack of reliable and specific markers. Here we identified the transcription factor PAX7 as a specific marker of a rare subpopulation of A_{single} spermatogonia in mice. PAX7$^+$ cells were present in the testis at birth. Compared with the adult testis, PAX7$^+$ cells constituted a much higher percentage of neonatal germ cells. Lineage tracing in healthy adult mice revealed that PAX7$^+$ spermatogonia self-maintained and produced expanding clones that gave rise to mature spermatozoa. Interestingly, in mice subjected to chemotherapy and radiotherapy, both of which damage the vast majority of germ cells and can result in sterility, PAX7$^+$ spermatogonia selectively survived, and their subsequent expansion contributed to the recovery of spermatogenesis. Finally, PAX7$^+$ spermatogonia were present in the testes of a diverse set of mammals. Our data indicate that the PAX7$^+$ subset of A_{single} spermatogonia functions as robust testis stem cells that maintain fertility in normal spermatogenesis in healthy mice and mediate recovery after severe germline injury, such as occurs after cancer therapy.

Introduction

The functional unit of the mammalian testis, the seminiferous tubule, is a multilayered epithelium that matures from spermatogonial precursors located at the basal layer to more advanced cell types that migrate toward the tubular lumen, where spermatozoa are released (1). Classically, type A_{single} spermatogonia, which reside on the basement membrane (i.e., the basal layer), were thought to represent the stem cell population of the testis, as these cells were the earliest identifiable morphological progenitors (2, 3). Meticulous histological studies have shown that A_{single} spermatogonia progress through multiple rounds of mitoses with incomplete cytokinesis to produce "chains" of A_{pair} and "aligned" A_{al4}, A_{al8}, and A_{al16} spermatogonia, which consist of 2, 4, 8, and 16 interconnected cells, respectively (4). A_{single}–A_{al16} spermatogonia are sometimes called "undifferentiated" spermatogonia, a term that is useful but also somewhat misleading, in that this population encompasses the true stem cells as well as a progressive series of differentiating, transit-amplifying intermediates. Interestingly, time-lapse imaging studies of mouse testes have clearly documented that A_{single}–A_{al16} spermatogonia are highly migratory, capable of moving across large distances on the basement membrane (5). A_{al16} spermatogonia differentiate to give rise to type A_1–A_4 and then to type B spermatogonia, which become spermatocytes that initiate meiosis. Round haploid spermatids, the products of meiosis, initiate a dramatic cytoskeletal rearrangement to produce elongate spermatids, which at the end of this maturational sequence are released within the tubular lumina as spermatozoa (Supplemental Figure 1; supplemental material available online with this article; doi:10.1172/JCI75943DS1; and ref. 6).

The continuous production of spermatozoa throughout adult life, as well as the multitude of cell divisions from A_{single} spermatogonia to mature spermatozoa, clearly implies the existence of a dynamic germline stem cell capable of self-maintenance, but also differentiation into the transit-amplifying intermediates that constitute the spermatogenic series (7). The identity of this adult testis stem cell remains unknown (8). As stated above, some models have posited that all A_{single} spermatogonia represent functional stem cells, consistent with their status as the earliest known morphological precursor. A_{single} spermatogonia can be reliably identified by morphologic criteria (i.e., their singularity by confocal microscopy of intact tubules) but have remained largely undefined at the molecular level, although recently ID4 was described as a marker of A_{single} spermatogonia (9). On the other hand, some studies have suggested that only a subset of A_{single} spermatogonia are functional stem cells (10). If so, then this would suggest that A_{single} spermatogonia encompass the true stem cells (a distinct fraction of A_{single} spermatogonia), along with other A_{single} subsets that serve as transit-amplifying descendants prior to their eventual differentiation to A_{pair} spermatogonia.

Transplantation of spermatogonia from a donor mouse to a germ cell–deficient recipient testis (11) has been extensively used to explore the properties and biology of spermatogonial stem cells

Conflict of interest: The authors have declared that no conflict of interest exists.
Submitted: March 3, 2014; **Accepted:** July 1, 2014.
Reference information: *J Clin Invest*. 2014;124(9):3929–3944. doi:10.1172/JCI75943.

(SSCs) (12). In these assays, the regeneration of complete spermatogenesis occurs via the formation of spermatogenic colonies thought to arise from a single transplanted cell. Clonogenicity is a notable strength of the assay, permitting assessment of stem cell numbers in the donor population. However, transplantation has not proven decisive in identifying the true (presumably rare) stem progenitors in the adult testis. Most strategies to enrich SSCs in transplantation assays to date have used cell surface selection markers such as THY1 (13) or α6/β10 integrins (14) that are expressed across broad subsets of spermatogonia, limiting their precision in pinpointing rarer subsets of stem progenitors (1, 8, 15). Furthermore, transplantation assays do not mirror stem cell functionality in the undisturbed testis. Donor germ cells are dissociated into single-cell suspensions, resulting in chain fragmentation, a phenomenon that occurs in vivo and has been proposed as a distinct mechanism promoting stem cell renewal, though this has not yet been conclusively demonstrated (5). Additionally, germ cells in the recipient are ablated by treatments that also damage the somatic environment, which may induce stemness by increasing the number of available niches or by eliminating negative feedback signals that emanate from other germ or somatic cells to regulate stem cell numbers within the testis (3, 16, 17).

A notable strength of the mouse testis as a model system for stem cell biology is the ability to establish cultured SSCs ex vivo. Cultured SSCs are capable of self-renewal and are truly immortal: they can be passaged and expanded indefinitely, maintaining genetic stability. The dynamics of stem cell maintenance in the murine SSC culture system are incompletely understood, but the cultures contain a much higher fraction of stem cells relative to the adult testis (18, 19). Cultured SSCs can be transplanted into a host testis, where they function as tissue stem cells, reestablishing functional spermatogenesis (20). The limitless expansion of SSCs in culture is dependent on the growth factor GDNF, which acts through the RET/GFRα1 receptor complex, although additional growth factors are also necessary (20–22).

Here we report on our identification of a rare subset of A_{single} spermatogonia characterized by expression of the paired box transcription factor PAX7. PAX7 has been previously identified and extensively used as a marker of satellite cells, which function as a normally quiescent stem cell population within adult skeletal muscle (23). In contrast, PAX7$^+$ spermatogonia were highly proliferative during steady-state spermatogenesis. To explore the contribution of PAX7$^+$ spermatogonia to normal spermatogenesis in the undisturbed testis, we performed a variety of cell lineage–tracing studies with an inducible *Pax7-Cre^{ERT2}* allele and 2 different reporters. These studies revealed that PAX7$^+$ spermatogonia normally serve as robust stem cells that contribute to full-lineage maturation, as evidenced by the formation of clones including all stages of spermatogenesis from A_{single} spermatogonia to spermatozoa. Furthermore, labeled (i.e., lineage-traced) descendants including A_{single} spermatogonia were observed even after prolonged intervals (16 weeks), which demonstrated that PAX7$^+$ spermatogonia function as bona fide stem cells that self-maintain and differentiate to sustain spermatogenesis, and are not merely transit-amplifying intermediates. Lineage-tracing studies with neonatal mice suggest that adult PAX7$^+$ spermatogonia are derived from an initial cohort of PAX7$^+$ spermatogonia present at birth. Finally, we conducted a number of investigations to explore the contribution of these rare PAX7$^+$ spermatogonia to spermatogenic recovery after germ cell ablation, such as occurs after chemotherapy or radiotherapy. Remarkably, PAX7$^+$ spermatogonia selectively survived cytotoxic drugs and radiation despite widespread germ cell death. Not only did their numbers not decrease in the immediate aftermath of such treatments, but instead, PAX7$^+$ spermatogonia rapidly expanded to replenish normal spermatogenesis. Thus, our results demonstrated that PAX7 spermatogonia are stem cells that maintain fertility in the healthy adult, and also serve particularly important roles in replenishing spermatogenesis following treatments that damage the germline.

Results

PAX7 specifically marks a small subset of A_{single} spermatogonia in vivo. We reasoned that a bona fide testis stem cell marker should be highly expressed in SSC cultures, but at low (perhaps undetectable) levels in the adult testis, where true stem cells are a rare subpopulation. An RNA-based approach previously used for marker discovery in ovarian cell subpopulations (24) led us to the identification of *Pax7* (Figure 1A). At the mRNA level, *Pax7* was highly expressed in SSC cultures, but undetectable in adult testis (>180-fold difference; Figure 1B). In vivo, *Pax7* transcripts were detectable in type A (early) spermatogonia, but not in differentiated type B spermatogonia, spermatocytes, or round spermatids. *Pax7* transcripts were absent in testes at embryonic days 11.5–18.5 (e11.5–e18.5) and first detected at postnatal day 2 (PD2). Among adult tissues, *Pax7* was expressed only in skeletal muscle, consistent with PAX7's eminence as a marker of satellite cells, the dormant tissue stem cell population that regenerates skeletal muscle after injury (23, 25). In comparison, the pan-germ cell marker *Ddx4* (also known as *VASA*) was expressed in adult testis (26) and in all germ cell subpopulations, but not in any somatic tissues, and transcripts were markedly decreased in germ cell–deficient (*Kitl^{Sl}/Kitl$^{Sl\text{-}d}$*) testes, as expected (Figure 1C). Thus, in contrast to *Pax7*, *Ddx4* did not exhibit a stem cell signature.

We sought to visualize PAX7$^+$ cells in sections of adult testis with an anti-PAX7 monoclonal antibody. PAX7$^+$ cells were rare: in 1 complete testis cross-section, a single PAX7$^+$ cell might be detected within seminiferous tubules (Figure 2A). Despite this rarity, several observations confirmed that the detection of PAX7$^+$ spermatogonia was specific, defining a novel population of spermatogonia. First, the PAX7$^+$ cells always rested on the basement membrane and were isolated, single cells (i.e., consistent with A_{single} spermatogonia; see also below). Second, PAX7 protein in spermatogonia was always nuclear, as expected based on its function and nuclear localization within satellite cells (23, 25).

To further define these PAX7$^+$ spermatogonia, we compared their abundance with that of other subsets of spermatogonia defined by well-characterized markers (Supplemental Figure 1). KIT$^+$ differentiating spermatogonia were the most abundant (10.9 cells/tubule), with FOXO1$^+$ and PLZF$^+$ spermatogonia being more restricted, as expected, given that FOXO1 and PLZF are both markers of undifferentiated (A_{single}→A_{al16}) spermatogonia, a less abundant population (27, 28). RET$^+$ spermatogonia were rarer still, consistent with RET's more restricted expression in A_{single} and A_{pair} spermatogonia (29). However, PAX7$^+$ spermatogonia were

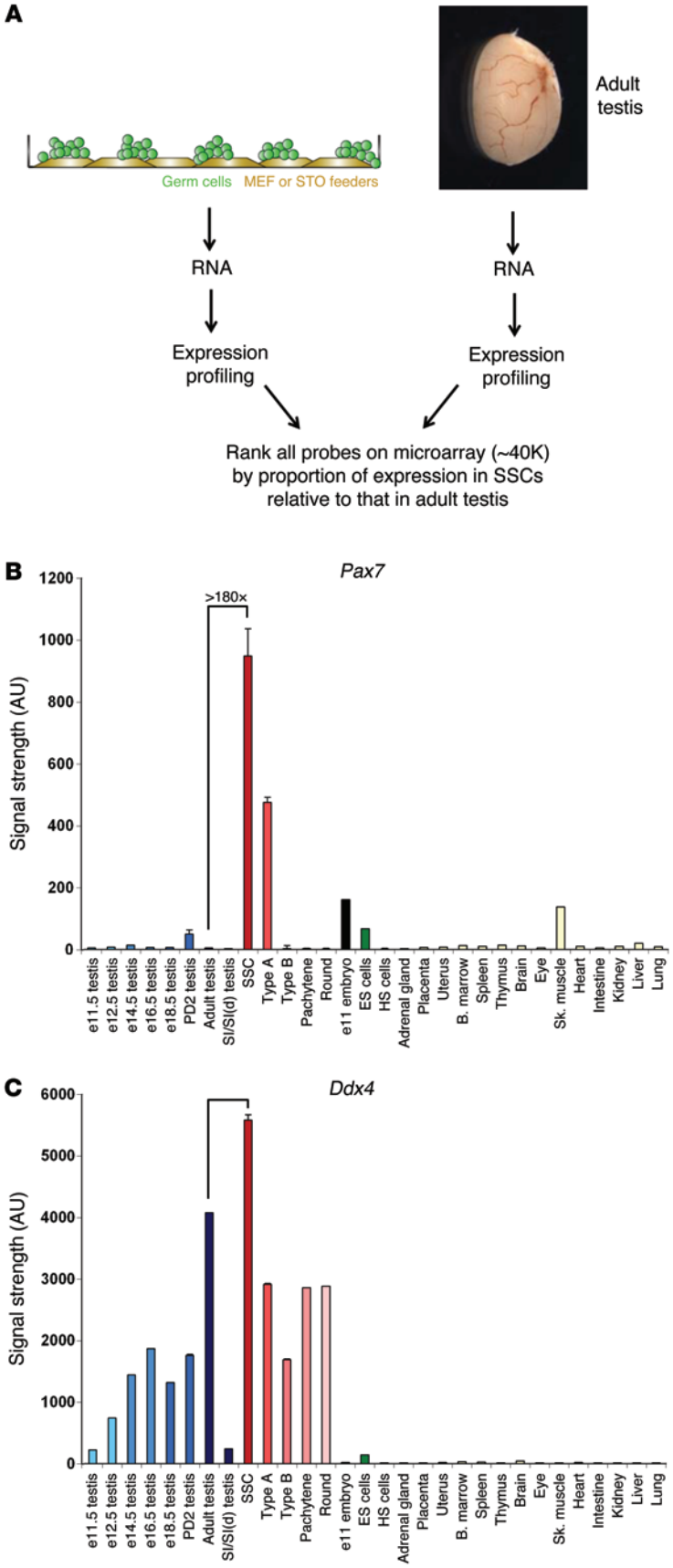

Figure 1. Digital Northern analysis identifying PAX7 as potential adult testis germline stem cell marker. (**A**) General RNA-based approach to identify markers that were highly expressed in cultured SSCs relative to adult testis. (**B** and **C**) Relative expression levels of (**B**) *Pax7* and (**C**) *Ddx4* across multiple samples. Error bars denote SEM. *Pax7* mRNA levels were >180-fold higher in established spermatogonial cultures relative to adult testis. SSC, cultured SSCs; Sl/Sl(d), $Kitl^{Sl}/Kitl^{Sl-d}$ germ cell–deficient adult testes; ES, embryonic stem; HS, hematopoietic stem.

approximately 2 orders of magnitude rarer than RET$^+$ spermatogonia (Figure 2B). PAX7$^+$ spermatogonia were FOXO1$^+$ and GFRα1$^+$, while most FOXO1$^+$ or GFRα1$^+$ cells were PAX7$^-$ (Figure 2C), which demonstrated that PAX7$^+$ spermatogonia represented a subset of undifferentiated, GFRα1$^+$ spermatogonia.

Confocal microscopy of intact seminiferous tubules further showed that PAX7$^+$ spermatogonia were a subset of A_{single} spermatogonia. PAX7$^+$ spermatogonia were singular, and larger chains of undifferentiated spermatogonia (i.e., A_{al4}–A_{al16}) never contained PAX7$^+$ spermatogonia (Figure 2D and Supplemental Video 1). Additional confocal microscopy studies confirmed that PAX7$^+$ spermatogonia were always KIT$^-$; no KIT$^+$PAX7$^+$ spermatogonia were ever observed (Figure 2E). Thus, PAX7 defined a rare but specific subset of A_{single} spermatogonia, revealing striking heterogeneity within A_{single} spermatogonia in vivo.

PAX7$^+$ spermatogonia are rare in the adult testis, but constitute a much higher fraction of germ cells in the neonatal testis. Interestingly, a much higher percentage of germ cells (defined by the pan–germ cell marker germ cell nuclear antigen [GCNA]) were PAX7$^+$ at birth (28% in neonates); however, this fraction steadily decreased postnatally, stabilizing at 6 weeks of age (Figure 3A). The much higher fraction of PAX7$^+$ germ cells at birth further underscores their rarity in adults, and also demonstrated that PAX7$^+$ spermatogonia can be reliably identified in tissue sections; analyses of conditional knockout testes also confirmed antibody specificity (see below).

This age-dependent decrease in the proportion of PAX7$^+$ cells per total GCNA$^+$ cells could reflect decreased absolute numbers of PAX7$^+$ spermatogonia, versus their dilution due to the massive expansion of spermatogenic cells that normally occurs during postnatal life (e.g., testes weights increase from ~1 mg at birth to ~60 mg in adult males) (30). To distinguish between these possibilities, we serially sectioned and immunostained entire PD1 and adult testes and documented similar numbers of PAX7$^+$ spermatogonia per testis (504 ± 29 and 402 ± 33, respectively; mean ± SEM; Figure 3B). Thus, the dramatic age-dependent decrease in the fraction of PAX7$^+$ germ cells reflects mainly the rapid expansion of spermatogenesis, and not a large decrease in absolute numbers of PAX7$^+$ cells. These results also strongly suggest that the postnatal PAX7$^+$ spermatogonia represent the initial founder population for PAX7$^+$ spermatogonia in adult testes.

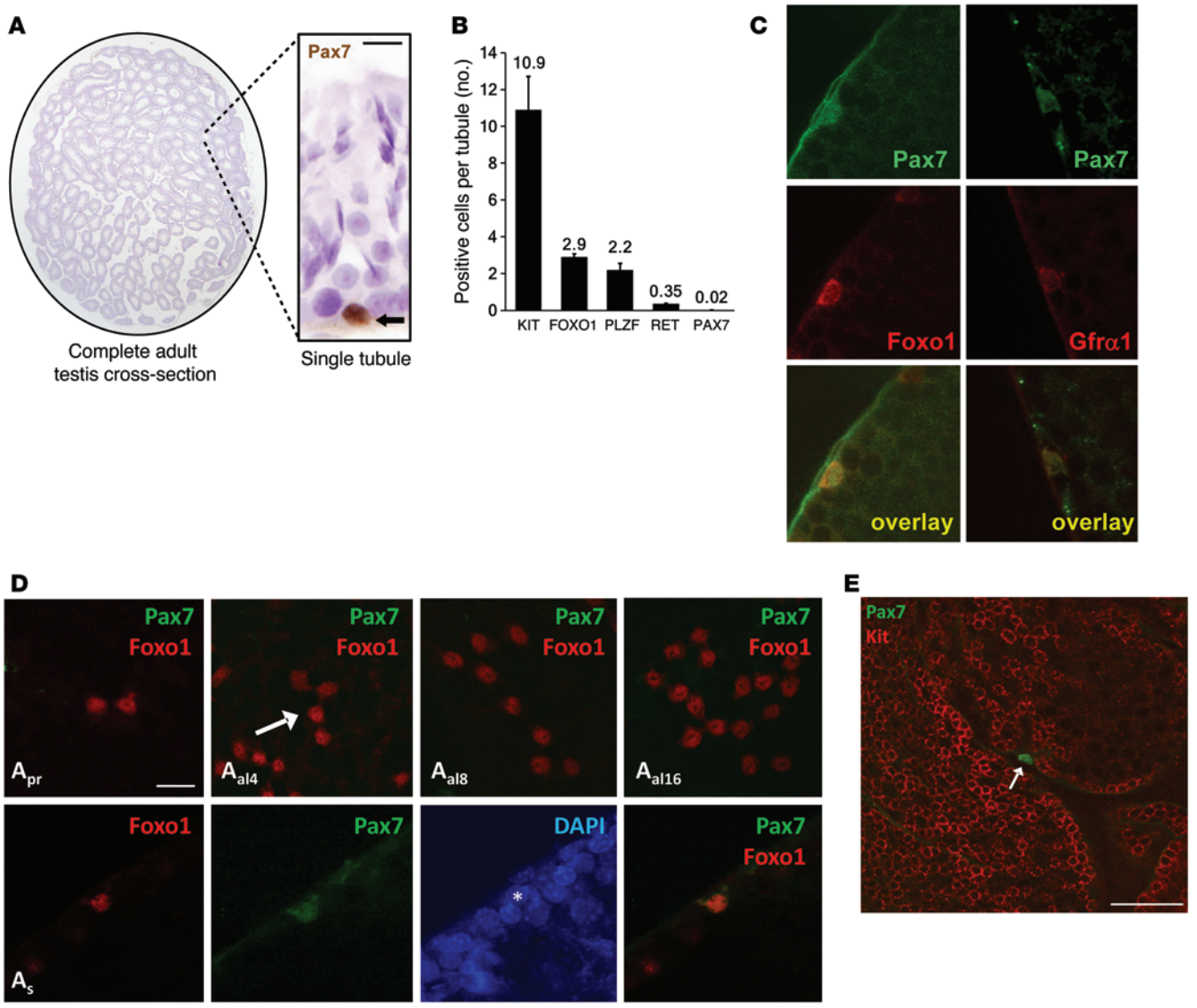

Figure 2. PAX7⁺ spermatogonia in normal testes. (**A**) Rarity of PAX7⁺ cells in adult (6-week-old) testis cross-section. Arrow denotes a PAX7⁺ cell within a single seminiferous tubule. (**B**) Relative number of spermatogonia positive for known markers compared with PAX7 in tissue sections, with >90 tubules counted per testis. Error bars denote SEM of averages derived from 3 6-week-old animals. (**C**) Double-labeling (confocal microscopy) showing that PAX7⁺ cells were FOXO1⁺ and GFRα1⁺ (representative examples among ≥10 PAX7⁺ cells). Basement membrane staining is nonspecific. (**D**) FOXO1 and PAX7 double-labeling of A_{single}, A_{pair}, and A_{al4}–A_{al16} chains, visualized by confocal microscopy. PAX7⁺ spermatogonia were A_{single} spermatogonia; larger chains did not contain PAX7⁺ spermatogonia. Arrow indicates an A_{al4} chain. Bottom panels show different channels for the same field of a single PAX7⁺FOXO1⁺ spermatogonium (asterisk in DAPI channel). (**E**) KIT and PAX7 double-labeling (confocal microscopy) showed that PAX7⁺ spermatogonia (arrow) were isolated (i.e., A_{single}) and KIT⁻. No KIT⁺PAX7⁺ spermatogonia were observed. PAX7 was nuclear, whereas KIT was membrane-associated, as expected. Image shows 3 tubules optically sectioned close to the level of the basement membrane to visualize large numbers of spermatogonia. Scale bars: 10 μm (**A**); 25 μm (**C** and **D**); 50 μm (**E**).

PAX7⁺ spermatogonia are rapidly cycling during normal spermatogenesis and function as robust stem cells that give rise to all stages of spermatogenesis. We considered the possibility that (by analogy with satellite cells) adult PAX7⁺ spermatogonia might represent a quiescent subset of A_{single} spermatogonia. To our surprise, however, EdU labeling showed that PAX7⁺ cells, like other subsets of spermatogonia, were rapidly cycling (Figure 3C).

We then sought to explore the contribution of PAX7⁺ spermatogonia and their descendants to normal, steady-state spermatogenesis in the undisturbed adult testis through lineage tracing. We used a *Pax7-Cre^{ERT2}* allele, in which the tamoxifen-inducible recombinase *Cre^{ERT2}* was knocked into the *Pax7* locus, driving *Cre^{ERT2}* expression in cells that express *Pax7*, such as satellite cells (Supplemental Figure 2A and refs. 31, 32). We generated mice harboring *Pax7-Cre^{ERT2}* and the *Rosa26* β-galactosidase *lox-stop-lox* reporter, *R26R* (33). 6-week-old adult males were treated with tamoxifen to activate Cre in PAX7⁺ cells. Untreated *Pax7-Cre^{ERT2};R26R* males exhibited no Cre-mediated recombination in testis or skeletal muscle, demonstrating tight control of Cre. Expression of PAX7 in labeled clones confirmed faithful *Pax7-Cre^{ERT2}* expression in PAX7⁺ spermatogonia (Supplemental Figure 2, B–D). To characterize PAX7⁺ descendants within the tes-

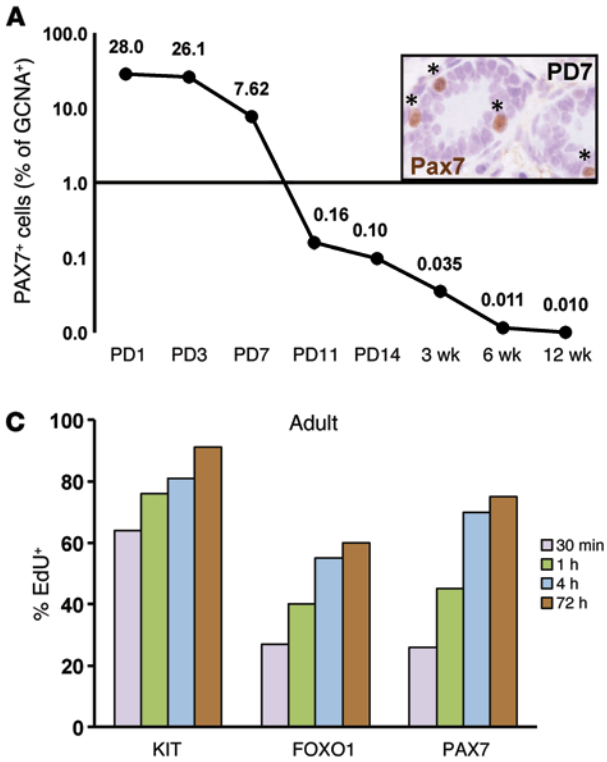

Figure 3. PAX7⁺ spermatogonia make up a higher percentage of germ cells in the neonatal testis. (**A**) PAX7⁺ cell frequency, expressed as a percentage of total GCNA⁺ cells. Inset: PAX7 IHC at PD7, showing several PAX7⁺ spermatogonia (asterisks). Magnification, ×250. (**B**) Counts of total PAX7⁺ cells by IHC of serially sectioned PD1 and adult testes (n = 3). Each bar represents a single testis. Total numbers were similar in neonatal and adult testes. (**C**) 6-week-old animals were injected with EdU, and testes were harvested after the indicated times. The experiment was repeated twice with similar results.

tis, labeled clones were analyzed after defined time intervals. By "clone," we refer not to individual spermatogonial chains, but rather to completely isolated groups of labeled cells that could constitute multiple chains, but were clearly descendants of a common progenitor — despite their sometimes complex arrangements — because of their close proximity. Notably, clones were very distant to their nearest neighbors and were much more isolated than the figures convey, with no labeled clones evident in either direction along the tubule. Thus, there is no question that these clones were separate tracing events at every time point analyzed.

At 4 days after tamoxifen treatment, clones were very small, most consisting of single, isolated cells, similar to the PAX7 immunostaining pattern (Figure 4A). The presence of slightly larger clones after 3 weeks and their subsequent rapid expansion was consistent with rapid cycling. There was striking clone expansion at successive time points, such that by 6 weeks of age, very large clones were readily visualized. Interestingly, larger clones were sometimes associated with distinctive "trails" of cells, some of which were clearly A_{single} spermatogonia based on their distance from other labeled descendants (i.e., multiple cell diameters; Figure 4A and Supplemental Video 1). This is indicative of complex patterns of migration of PAX7⁺ cells and their descendants, but could also reflect chain fragmentation. Labeled elongate spermatid tails were first identified 6 weeks after induction (Figure 4, B and C). Average clone size (i.e., number of cells per clone) increased over time, but clone numbers remained stable over this prolonged interval. This argues that PAX7⁺ spermatogonia are bona fide stem cells. If PAX7⁺ spermatogonia were instead transit-amplifying intermediates, labeled cells would become diluted out with time and eventually disappear, because the total duration of spermatogenesis (i.e., from A_{single} spermatogonium to sperm release) is only 39 days in the mouse (34).

Lineage-tracing experiments with *Pax7-Cre^{ERT2}* and a double-fluorescent tdTomato/eGFP reporter (*mT/mG*) (35) gave nearly identical results. Clones began as single cells. At 1 week after Cre induction, labeled A_{single}, A_{pair}, and A_{al4}–A_{al8} chains were identified. At 6 weeks, larger clones were visualized, and elongate spermatid tails were first identified in tubular lumina. By 16 weeks, clones were even larger (Figure 5A), and motile labeled sperm were present in epididymides (Supplemental Video 2). Labeled A_{single} spermatogonia were observed at all time points (Figure 5A and Supplemental Videos 3 and 4). To more clearly delineate clonal architecture, we also analyzed frozen tissue sections of intact testes, which permitted better visualization of spermatogenic layers and cell types. In some clones, all of the germ cells in the entire tubular cross-section were clearly labeled (green; Figure 5B), which demonstrated that all the germ cells (spermatogonia, spermatids, and spermatocytes) were derived from a PAX7⁺ progenitor. These results indicated that PAX7⁺ spermatogonia give rise to full-lineage maturation (Figure 5C), thereby fulfilling a key criterion of an adult testis stem cell. As with *R26R*-based lineage tracing, clone numbers did not decrease, even when the analyses were extended to 16 weeks after tamoxifen treatment (Figure 5, D and E). We concluded from these analyses with 2 distinct reporters that PAX7⁺ spermatogonia are rare but robust tissue stem cells. They give rise to other A_{single} spermatogonia that persist even after very long intervals of 16 weeks, and also give rise to all stages of spermatogenesis, including motile sperm.

Lineage-tracing studies of neonatal animals show that neonatal PAX7⁺ spermatogonia have long-term stem cell potential in vivo and also have stem cell activity in transplantation assays. Lineage-tracing studies initiated with neonatal animals (PD1–PD3) confirmed that PAX7⁺ spermatogonia were rapidly expanding by PD3 and

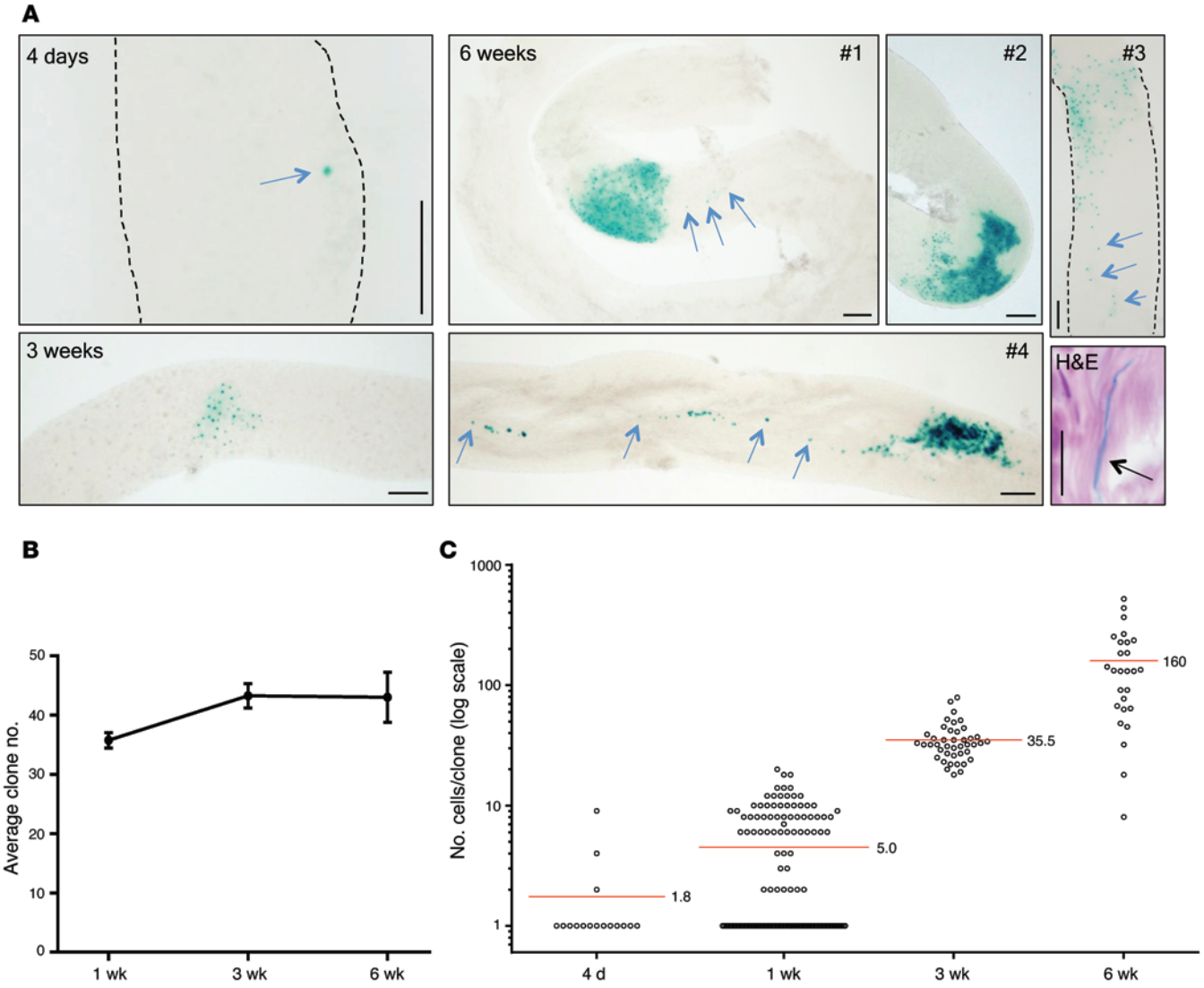

Figure 4. Lineage tracing of PAX7⁺ descendants in *Pax7-Cre^{ERT2};R26R* testes. Mice were treated with tamoxifen at 6 weeks of age then aged for the indicated intervals. (**A**) Representative clones at 4 days, 3 weeks, and 6 weeks. Dashed lines demarcate tubule borders. Arrows denote a 1-cell clone at 4 days or isolated A_{single} spermatogonia at the periphery of larger clones at 6 weeks. All marker-expressing cells in these fields are considered clonal because there were no additional marked cells in the tubule. The H&E-stained section of Xgal-treated testis at 6 weeks showed a single-labeled (blue) elongate spermatid tail among many unlabeled (pink) spermatid tails in the tubular lumen. Other labeled spermatid tails were outside the field of view. Scale bars: 100 μm; 10 μm (H&E). (**B**) Average clone numbers in $n = 4$ testes. The 1-week time point may represent undercount due to difficulty in visualizing single-cell clones, or marker expression lag. Clone numbers were consistent with the presence of approximately 400 PAX7⁺ cells per testis and 10% recombination efficiency for *Pax7-Cre^{ERT2}* after tamoxifen administration (31). (**C**) Clone size. Red bars denote means. Larger clones were composed of large labeled zones and peripheral smaller chains including A_{single} spermatogonia.

were progenitors of subsequent A_{single} spermatogonia and spermatogenesis; clones grew in size over time and persisted into adulthood (Figure 6, A and B). Concordantly, PAX7⁺ spermatogonia were rapidly proliferating by PD3, as shown by EdU incorporation rate, without significant cell death (Figure 6C). Finally, although flow sorting of live PAX7⁺ spermatogonia was not possible with available reagents, transplantations were conducted with unsorted cells from tamoxifen-treated *Pax7-Cre^{ERT2};tdTomato* reporter mice (36). Labeled, lineage-traced germ cells were observed in every host ($n = 3$; Figure 6D), which indicated that PAX7⁺ spermatogonia and their descendants have stem cell activity in transplantation assays.

PAX7⁺ spermatogonia are selectively resistant to anticancer therapies that kill other germ cells in the adult testis (radiotherapy and chemotherapy) and also contribute to spermatogenic recovery after ablation of most germ cells. Spermatogenesis is highly sensitive to systemic genotoxic stresses, such as cytotoxic chemotherapy. Chemotherapy-induced ablation of germ cells has been studied in rodent models. After treatment with the alkylating agent busulfan (also known as Myleran; used to treat hematopoietic malignancies), germ cells undergo massive cell death in a dose-dependent manner, with higher doses leading to near-total germ cell depletion. This results in an interval of azoospermia and infertility, followed by a gradual recovery of spermatogenesis and, in most

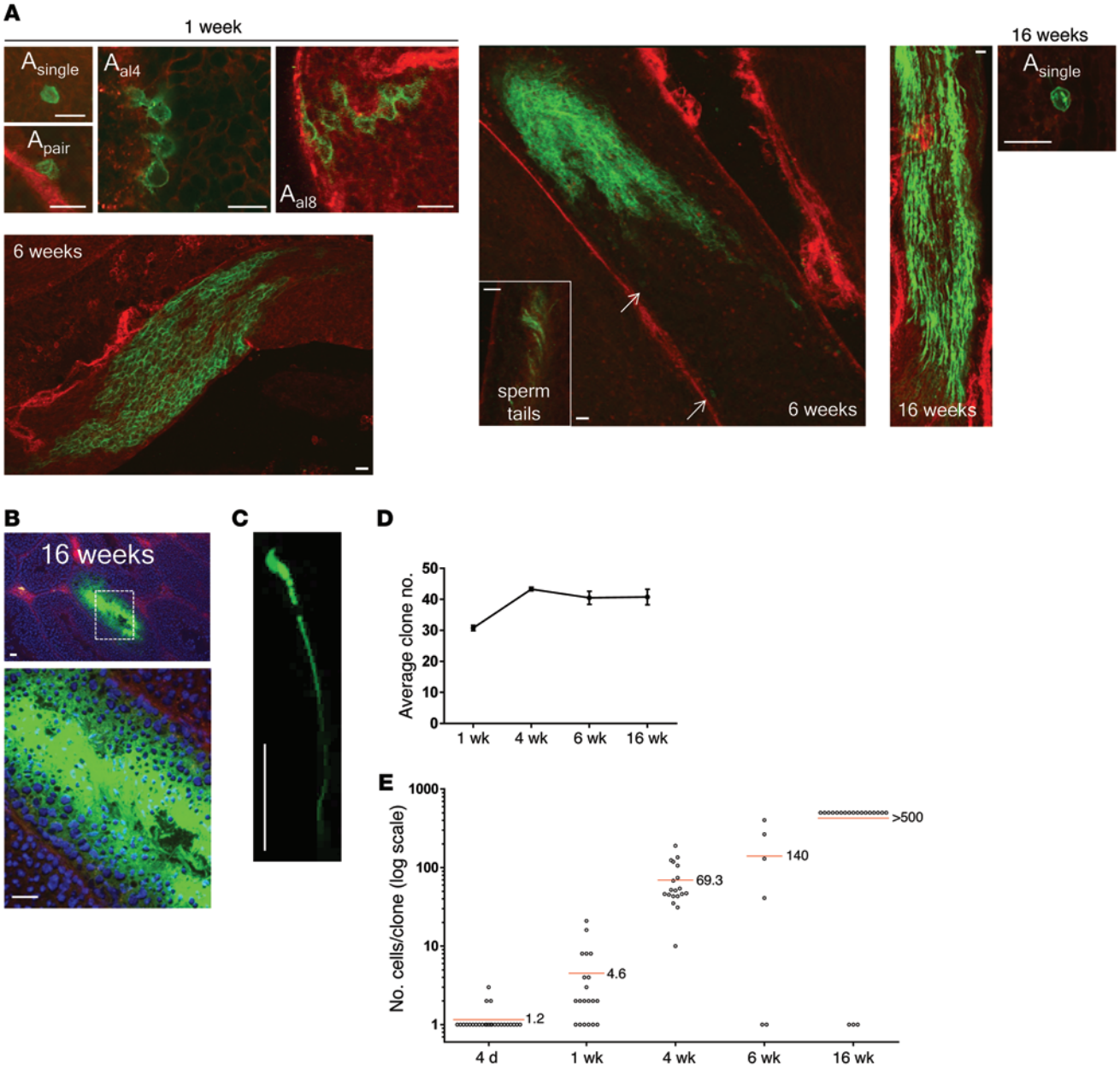

Figure 5. Lineage tracing of PAX7⁺ descendants in *Pax7-Cre^{ERT2};mT/mG* testes. Adult males were treated with tamoxifen at 6 weeks of age, then aged for the indicated intervals. (**A**) Clone morphology by confocal microscopy of isolated tubules. Representative A_{single}, A_{pair}, A_{al4}, and A_{al8} clones 1 week after tamoxifen administration are shown. Other panels show larger clones at 6 weeks; arrows indicate detached A_{single} spermatogonia that were part of larger clones. Inset: elongated spermatid tails in tubular lumen. Clones >500 cells could not be reliably counted. Larger clones were associated with smaller separate chains at their periphery, including A_{single} spermatogonia. The few 1-cell clones at 6–16 weeks represent A_{single} spermatogonia too distant from the nearest clone to be confidently identified as part of it, but may reflect long-distance migration. Green motile sperm were observed in the epididymis. (**B**) Clone morphology in tissue sections (16 weeks after tamoxifen). PAX7⁺ descendants gave rise to all spermatogenic stages, as evidenced by circumferential full-thickness labeling of all spermatogenic stages throughout the tubule. Tissue sections were counterstained with DAPI. (**C**) Labeled sperm from epididymis showing bright green fluorescence and characteristic hook morphology. The majority of sperm did not exhibit fluorescence, and control epididymides did not contain spermatozoa with comparable fluorescence (i.e., the signal shown is not background autofluorescence of sperm). (**D**) Average clone number in $n = 4$ testes. Clone numbers did not decrease over time. (**E**) Clone size. Red bars denote means. Larger clones included detached smaller chains and A_{single} spermatogonia. Scale bars: 25 μm.

animals, restoration of fertility even after high doses (37). Such spermatogenic recovery poses a paradox: the germline is almost entirely ablated, yet the restoration of spermatogenesis implies the existence of rare stem cells that not only survive, but replenish spermatogenesis during the recovery period (38).

To study the contribution of PAX7⁺ spermatogonia to spermatogenic recovery, adult mice (6 weeks of age) were treated with busulfan. As expected, testes underwent massive germ cell death with dose- and time-dependent germ cell loss, as visualized by immunohistochemistry (IHC) with the pan–germ cell

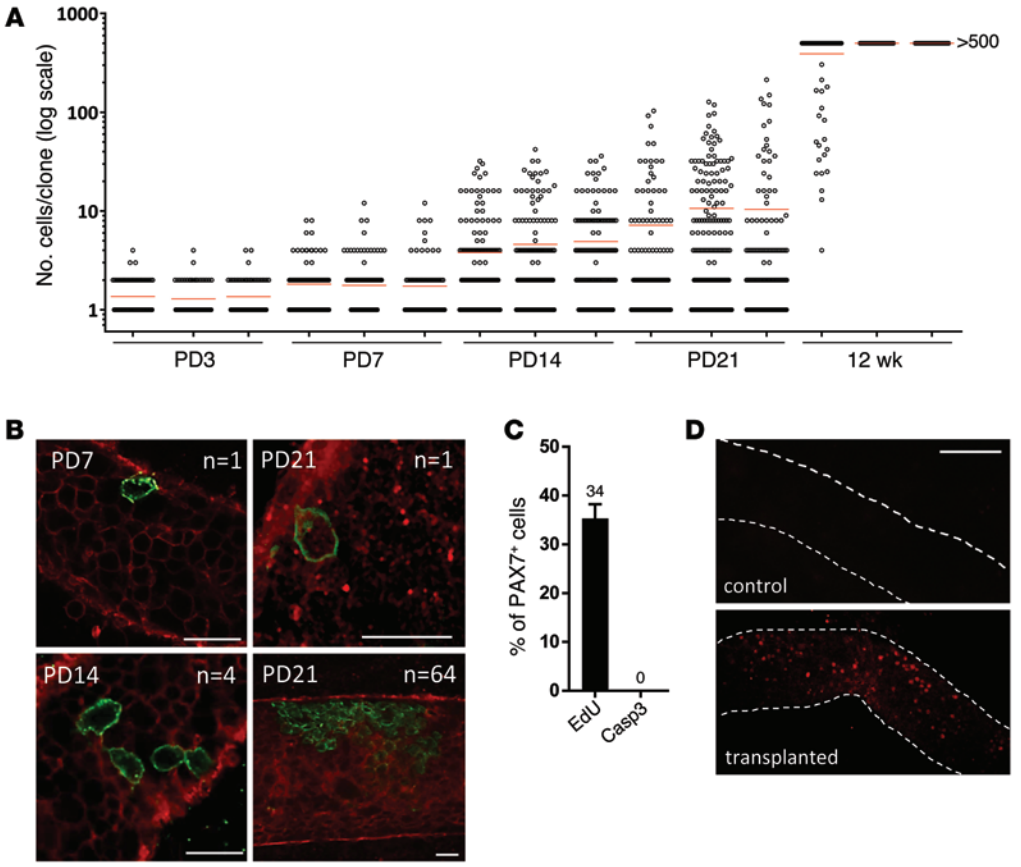

Figure 6. PAX7⁺ spermatogonia have long-term stem potential in vivo, and their descendants function as stem cells in transplantation assays. For PD3 time points, tamoxifen injections were performed at PD1 and PD2; for later time points, tamoxifen administration was performed for 3 consecutive days starting at PD3. (**A**) Clone size. Each column represents 1 testis from separate animals (total $n = 15$); red bars denote means. Note that many labeled A_{single} spermatogonia were present at PD21, demonstrating that PD21 PAX7⁺ spermatogonia are derived from neonatal PAX7⁺ spermatogonia. Clones grew over time and persisted in aged animals (12 weeks). (**B**) Representative clone morphologies by confocal microscopy (n denotes number of cells in labeled chain shown); z stacks confirmed cell counts and A_{single} status. (**C**) Mitotic and apoptotic indices of PAX7⁺ cells at PD3 ($n = 3$ animals) demonstrated that early PAX7⁺ cells were highly proliferative and not characterized by significant apoptosis. Error bars denote SEM. (**D**) Transplantation assay. A *Pax7-Cre^{ERT2};tdTomato* donor was treated with tamoxifen at PD3. Testes were disaggregated at PD14 and transplanted into germ cell–deficient *Kit^{W}/Kit^{W-v}* hosts, which were sacrificed after 4 weeks ($n = 3$). All hosts (but no controls) showed multiple labeled clones (i.e., 15–20); representative examples are shown. Scale bars: 25 μm (**B**); 100 μm (**D**).

marker GCNA (39). In striking contrast, both relative and absolute numbers of PAX7⁺ spermatogonia increased several-fold, also in a time- and dose-dependent manner (Figure 7A). Absolute numbers of PAX7⁺ cells peaked (>5-fold higher than untreated mice) 16 days after treatment with the highest dose of busulfan (40 mg/kg). PAX7⁺ cell counts then decreased between 16 and 32 days, most likely a consequence of differentiation (see below). Thus, while germ cells as a whole were largely ablated by busulfan, PAX7⁺ cells not only survived, but expanded in number.

Histology and immunostaining confirmed massive loss of germ cells. Whereas in untreated animals, virtually all PAX7⁺ cells were single, isolated cells (with only extremely rare cells being present as pairs, and never in clusters of ≥3), larger PAX7⁺ clusters of 2 to ≥4 cells were observed after busulfan treatment (Figure 7, B and C). This difference in cluster sizes (1 versus ≥2) was highly statistically significant in untreated animals versus those 32 days after treatment with 40 mg/kg busulfan ($P = 2 \times 10^{-9}$). The PAX7⁺ fraction undergoing DNA replication, based on EdU incorporation, increased 4 days after busulfan treatment (Figure 7D), demonstrating that busulfan treatment stimulated PAX7⁺ cell division acutely and suggesting that cell division is one mechanism underlying the formation of PAX7⁺ cell clusters. In contrast to PAX7⁺ spermatogonia, FOXO1⁺ undifferentiated spermatogonia counts fell more than 15-fold 8 days after 40 mg/kg busulfan administration, but then recovered coincident with the peak of PAX7⁺ expansion (Figure 8A). These data indicate that spermatogonia are sensitive to genotoxic stress as previously reported (40), emphasizing the unique properties and survival of PAX7⁺ spermatogonia after treatments that ablate the vast majority of germline cells. That the increase in FOXO1⁺ spermatogonia coincided with the decrease of PAX7⁺ spermatogonia (Figure 8, B and C) is further evidence that PAX7⁺ spermatogonia eventually differentiate. In control experiments, neither tamoxifen nor the DMSO solvent had a significant effect on testis weight or morphology or PAX7⁺ spermatogonia (Supplemental Figure 3, A–D).

We then analyzed the response of PAX7⁺ spermatogonia to ionizing radiation and a second chemotherapeutic agent commonly used in the clinic, cyclophosphamide. Cyclophosphamide

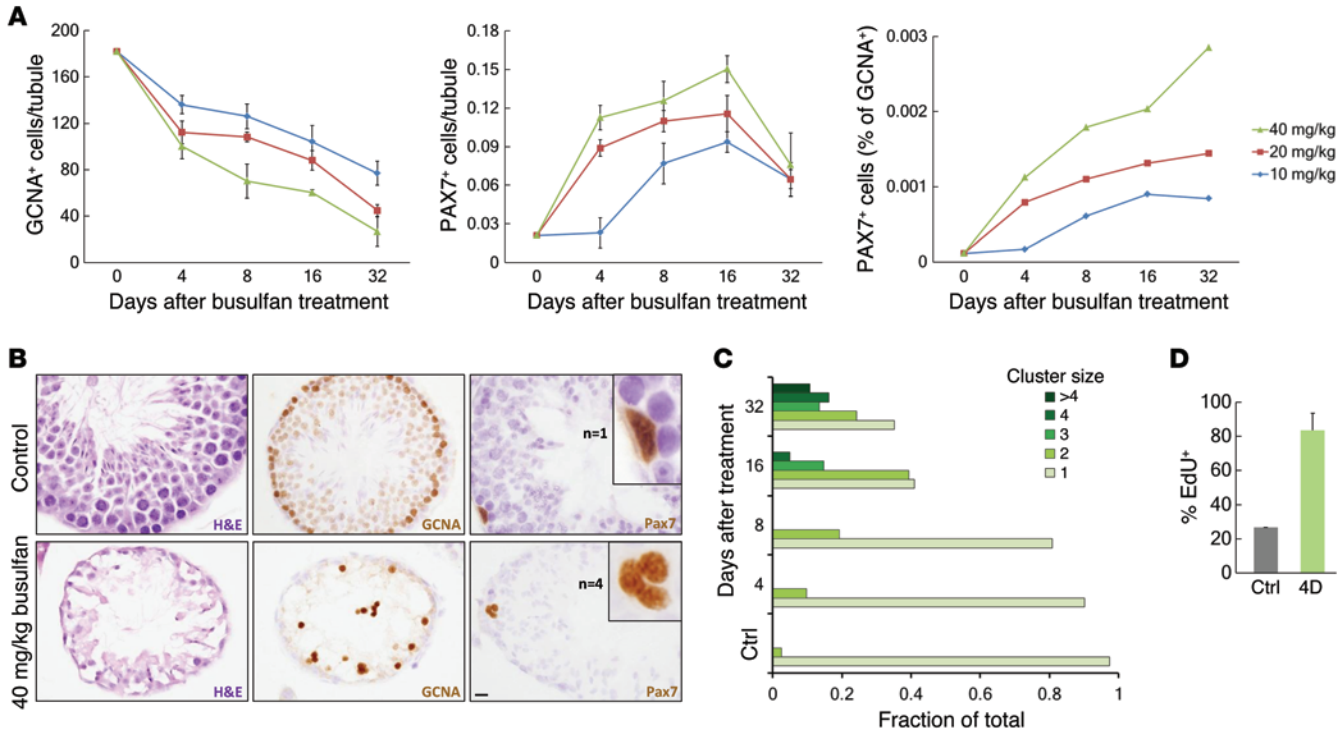

Figure 7. Germline ablation with busulfan has dose-dependent effects on PAX7⁺ spermatogonia. (**A**) Number of cells expressing GCNA (pan-germ cell marker) and PAX7. Error bars denote SEM for $n = 3$ animals at 6 weeks of age. (**B**) H&E and immunostained sections 16 days after a single dose of 40 mg/kg busulfan. GCNA stains all germ cells to the round spermatid stage. Busulfan resulted in expansion of PAX7⁺ clusters never observed in untreated testes; an example of a 4-cell group is shown (insets; enlarged ×4). (**C**) Fractions of PAX7⁺ clusters of different sizes. For each time point, fractions add up to 1. The difference in cluster sizes (1 versus ≥2) was highly statistically significant in untreated animals versus those treated with 40 mg/kg busulfan after 32 days ($P = 2 \times 10^{-9}$). (**D**) Percent EdU incorporation in PAX7⁺ spermatogonia 4 days after busulfan administration. Scale bar: 10 μm.

is less toxic to the germline, necessitating a longer treatment protocol (150 mg/kg i.p. every 5 days for 25 days) than busulfan, which was administered as a single dose. Radiation was administered in a single (nonfractionated) dose of 5 Gy. Selective survival and clustering of PAX7⁺ spermatogonia ($P < 10^{-5}$) similar to that observed after busulfan were also observed after either external irradiation or cyclophosphamide (Supplemental Figures 4 and 5). After cessation of each treatment, the number of PAX7⁺ spermatogonia increased, then subsequently declined, as was observed with busulfan. These results are significant in that they demonstrate that in the mouse, PAX7⁺ spermatogonia selectively survive first-line cancer therapies that often result in reversible or permanent sterility in men and boys (41). These findings make PAX7⁺ spermatogonia strong candidates as the "spermatogenic recovery" cells postulated to be responsible for the restoration of fertility after cytotoxic/genotoxic treatments in rodent models (42).

To further explore this possibility, lineage-tracing studies were performed with adult mice treated with 20 mg/kg busulfan. In the first experiment, lineage tracing was initiated by tamoxifen (usual 3-day regimen) followed by busulfan (referred to herein as the tam→bu protocol). In a second experiment, the order of treatments was reversed, and tamoxifen was administered 15–17 days after busulfan administration, the time point coinciding with the peak of PAX7⁺ cells (bu→tam protocol; Figure 9A). In each experiment, PAX7⁺ spermatogonia contributed to spermatogenic recovery, as evidenced by the presence of labeled clones 8 weeks after the last treatment. With the tam→bu protocol, the number of clones was fewer than in untreated control mice ($P = 0.002$), whereas the number of clones was greater than controls in the bu→tam protocol ($P = 0.021$). These results were consistent with the expansion of PAX7⁺ cells observed at 16 days after busulfan (Figure 7A and Figure 9, B and C). The somewhat smaller mean clone sizes in the bu→tam versus tam→bu experiments (161 vs. 378 clones) could be explained by the administration of tamoxifen 15–17 days after busulfan, whereas in the tam→bu protocol, busulfan was administered only 8 days after tamoxifen. This 7- to 9-day difference might permit 1 or more additional cell doublings to occur in the tam→bu protocol, thus accounting for the modestly increased clone size (~2-fold difference). Clone morphology was similar to that observed in the prior lineage-tracing experiments; an example of a large clone is shown in Figure 9D. In tissue sections of the larger clones, the labeled cells made up all of the germ cells in a tubular cross section (Figure 9E), demonstrating that, as in normal spermatogenesis in untreated mice, PAX7⁺ spermatogonia contributed to full-lineage maturation after busulfan treatment. Together, these data showed that PAX7⁺ spermatogonia not only selectively survive, but also contribute to the reestablishment of spermatogenesis after diverse genotoxic insults to the germline, including radiotherapy and chemotherapy (38).

Preliminary observations demonstrate that PAX7 is dispensable for spermatogenesis. To study the genetic requirements for *Pax7* in spermatogenesis, we performed conditional genetic knock-

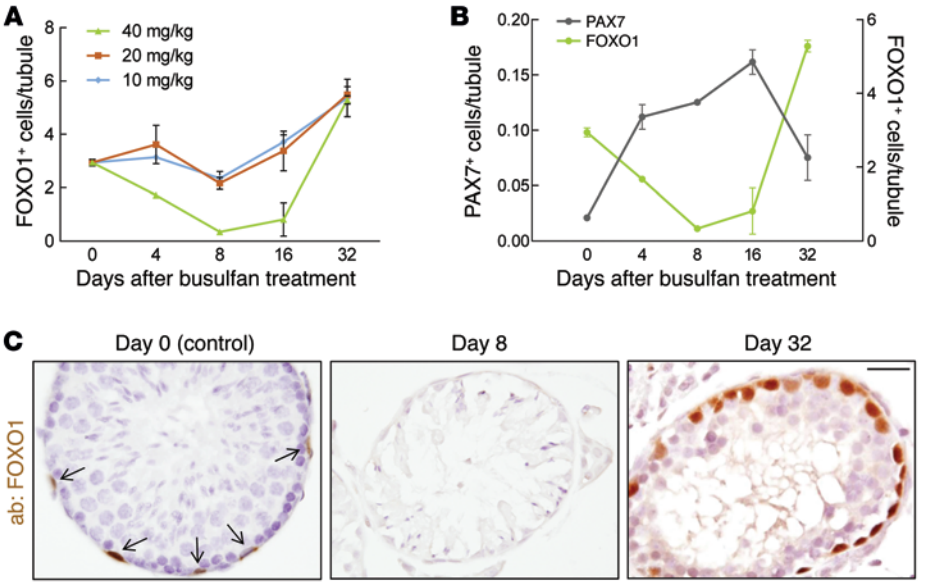

Figure 8. Counts of FOXO1⁺ spermatogonia after busulfan administration at 6 weeks of age. For each time point, *n* = 3 animals were analyzed; error bars denote SEM. (**A**) FOXO1⁺ spermatogonia per tubule. (**B**) FOXO1⁺ counts per tubule compared with PAX7⁺ counts. (**C**) IHC showing FOXO1⁺ spermatogonia (arrows). Unlike PAX7⁺ spermatogonia, FOXO1⁺ (undifferentiated) spermatogonia were not resistant to busulfan. Scale bar: 25 μm.

out (cKO) with the germline-specific *VASA-Cre* (*VC*), which we had previously generated and characterized (43), and a conditional (floxed) *Pax7*^{fl} allele (32). The resulting *Pax7* germline cKO mice (*VC;Pax7*$^{-/fl}$) had testes that were morphologically normal and exhibited normal spermatogenesis, as evidenced by normal weights and histological analyses. Furthermore, all males (*n* = 3) were fertile, with normal litter sizes (Figure 10, A–D), which indicated that *Pax7* is dispensable for male fertility in mice. *Pax7* cKO males treated with busulfan (*n* = 3) showed a significant lag in spermatogenic recovery 8 weeks after treatment (Supplemental Figure 6), although this lag was somewhat variable. In *Pax7* cKO males, testes showed a trend toward smaller size (*P* = 0.25), but many tubules lacked complete spermatogenesis, while in control animals, practically all tubules had recovered (*P* = 0.016).

The availability of *Pax7* cKO testes permitted us to confirm the specificity of PAX7 immunodetection. Whereas intratubular germ cells were readily detectable by GCNA immunostaining of control and *Pax7* cKO testes, PAX7 expression was abolished in *Pax7* cKO testes compared with wild-type controls (Figure 10E), confirming the specificity of PAX7 immunodetection. Thus, *Pax7* appears to be dispensable for spermatogenesis, at least in the laboratory setting, but may make a functional contribution to the recovery of spermatogenesis under conditions of germline stress (see Discussion).

PAX7⁺ spermatogonia are present across mammalian species. We sought to determine whether PAX7⁺ spermatogonia are phylogenetically conserved in spermatogenesis, as many aspects of spermatogenesis are shared by diverse species (44–47). The monoclonal antibody we used to detect PAX7⁺ spermatogonia was generated against chicken PAX7 (*Gallus gallus*; amino acid [aa] 300–523), which suggests that the epitope might be broadly conserved (48). However, there was no a priori guarantee that this would be the case. We epitope-mapped the anti-PAX7 monoclonal antibody with a tiled peptide array of both the chicken and corresponding mouse aa sequences at 1-aa resolution. This identified a distinct 10-aa peak at identical positions in the chicken and mouse polypeptides (Figure 11A). Western blotting with a 22-aa blocking peptide spanning this epitope effectively eliminated the PAX7 signals (but not nonspecific background bands; Figure 11B), which confirmed that this was the epitope detected by the PAX7 monoclonal antibody. Alignment of corresponding aa sequences from diverse species revealed that the 10-aa PAX7 epitope is conserved across all 11 mammalian PAX7 homologs evaluated, but not in the zebrafish (*Danio rerio*) or the fruit fly (*Drosophila melanogaster*) (Table 1). We then performed immunolocalization of PAX7 in tissue sections of paraffin-embedded, formalin-fixed testes from diverse mammalian species, including companion and domestic animals, nonhuman primates, and humans. Rare basal PAX7⁺ spermatogonia were present in these species (Figure 11C). Interestingly, PAX7⁺ cells were more abundant in juvenile testes (which were available for cat and baboon), with multiple cells in some tubules, similar to our observations in mice. These results suggest that PAX7⁺ spermatogonia serve important roles as adult testis stem cells and contribute to spermatogenesis in a wide range of species.

Discussion

Our data revealed surprising heterogeneity in cells previously identified through morphologic criteria as A_{single} spermatogonia. This finding also suggests the existence of further A_{single} subtypes, which may be characterized by the expression of other distinct markers, such as ID4 or ERBB3 (9, 49, 50). PAX7 defined an unexpectedly small subset of A_{single} spermatogonia. PAX7⁺ spermatogonia were highly proliferative in steady-state spermatogenesis and fulfilled criteria of self-renewal and complete lineage differentiation in the adult testis. That PAX7 is a marker of germline stem cells in the testis is notable in light of extensive studies of PAX7 as a marker of satellite cells (23, 25). Our work shows some commonalities between PAX7⁺ stem cells in the testis and skeletal muscle, but also some important differences. PAX7⁺ cells were rarer in the testis, making them difficult to detect. In skeletal muscle, a tissue characterized by little cellular proliferation, PAX7⁺ cells are normally quiescent, only to become reactivated after injury. In contrast, in the testis, PAX7⁺ spermatogonia were highly proliferative and continually replenish spermatogenesis.

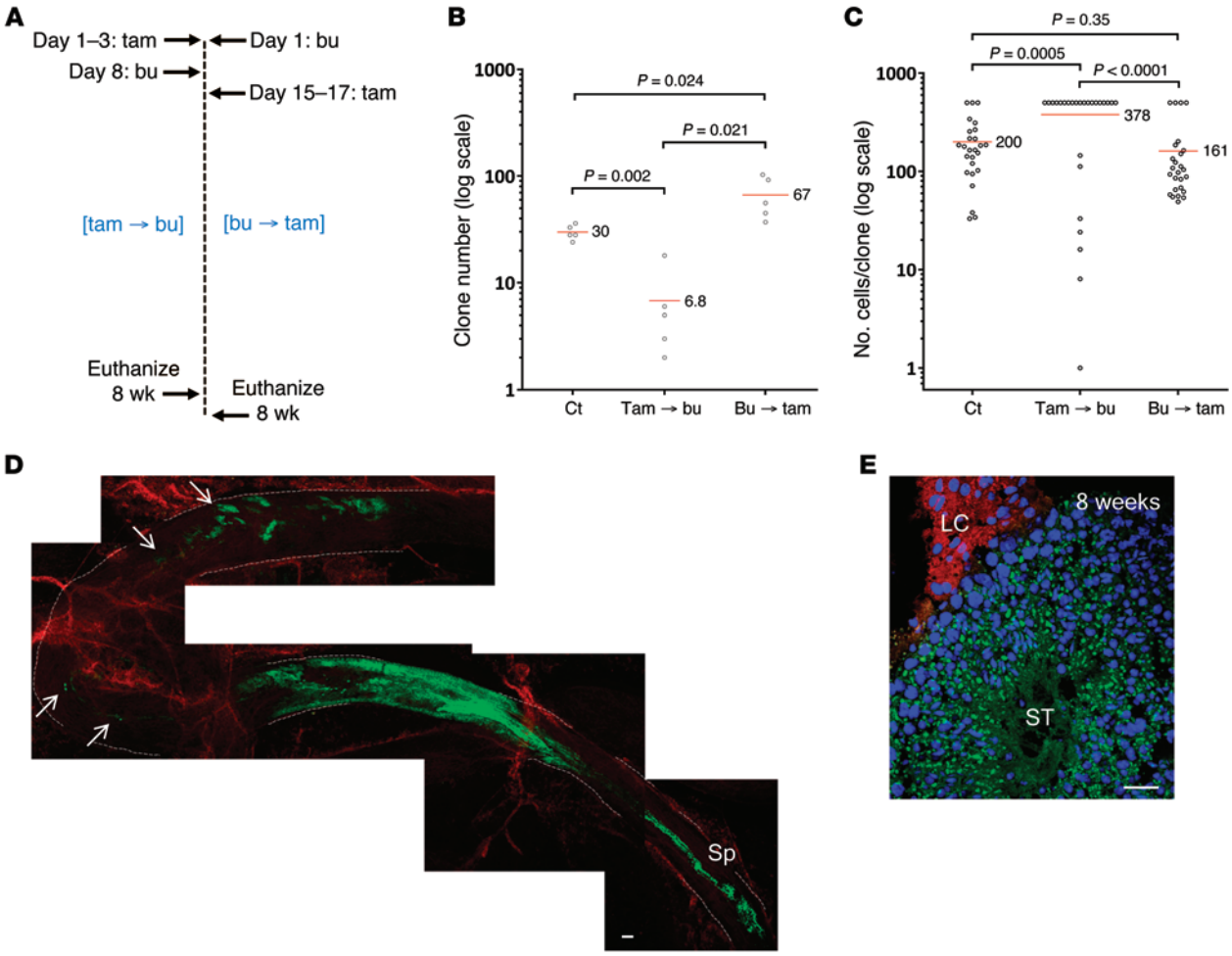

Figure 9. Lineage tracing of PAX7⁺ spermatogonia following busulfan (20 mg/kg) treatment of *Pax7-Cre^{ERT2};mT/mG* males at 6 weeks of age. (**A**) Schematic showing both busulfan lineage-tracing experiments. Testes were harvested 8 weeks after the last drug dose for each experiment. (**B**) Number of clones 8 weeks after busulfan administration. Each point represents 1 testis from 1 animal; red bars denote means; *P* values were determined by unpaired *t* test. (**C**) Clone size 8 weeks after tamoxifen administration. Red bars denote means; *P* values were determined by unpaired *t* test. (**D**) Composite image of representative large clone from tam→bu experiment. Tubule borders are highlighted with dashed lines. Sp, elongate spermatids (arrows denote individual cells or small groupings forming a "trail" of cells). (**E**) Cryosection of testis from tam→bu experiment showing germ cell clone spanning the entire tubule. ST, seminiferous tubule; LC, Leydig cells. Scale bar: 200 μm (**D**); 25 μm (**E**).

PAX7 as a testis stem cell marker. Our data are consistent with a model whereby PAX7⁺ A_{single} spermatogonia function as stem cells in the adult testis. The fact that only a minority of A_{single} spermatogonia were PAX7⁺ indicated that the A_{single} population is more heterogenous that some models propose, although elegant studies previously suggested that only a subset of A_{single} spermatogonia function as true stem cells (8, 10). Our present findings indicate that the fraction of A_{single} spermatogonia that are PAX7⁺ is in the range of 1% to 10% (3). We speculate that PAX7⁺ spermatogonia sit at the top of the differentiation hierarchy, further suggesting that there are other subsets of A_{single} spermatogonia — perhaps defined by currently unknown markers — that function as transit-amplifying intermediates prior to differentiating to A_{pair} spermatogonia (Figure 12). However, other models are possible (5, 17), necessitating future investigations to gain a complete understanding of the cellular hierarchies underlying stem cell maintenance and differentiation in the mammalian testis.

Some have argued that SSC transplantation represents a gold standard and is the only reliable assay for studying testis stem cell activity. Reconstitution of a self-maintaining cellular clone in a host organ is indisputable evidence that the cell of origin functioned as a stem cell in the assay. However, other investigators in the stem cell field have challenged the assumption that transplantation assays recapitulate stem cell function in native, undisturbed organs, and have pointed out limitations inherent in transplantation assays (51). These concerns are valid for SSC transplantations (5, 8, 16, 17), particularly since transplantation requires treatments (cell dissociation in the donor, near-complete germ cell ablation in the host) that may strongly stimulate regenerative potential in ways that are not fully understood. There is an important distinction to be made between actual stemness and the potential for stemness. Transplantation assays are clearly useful for studying the latter, but do not necessarily accurately reflect the former (51). Future investigations are needed to define plasticity with respect to actual stemness versus stemness potential (52) in the adult testis.

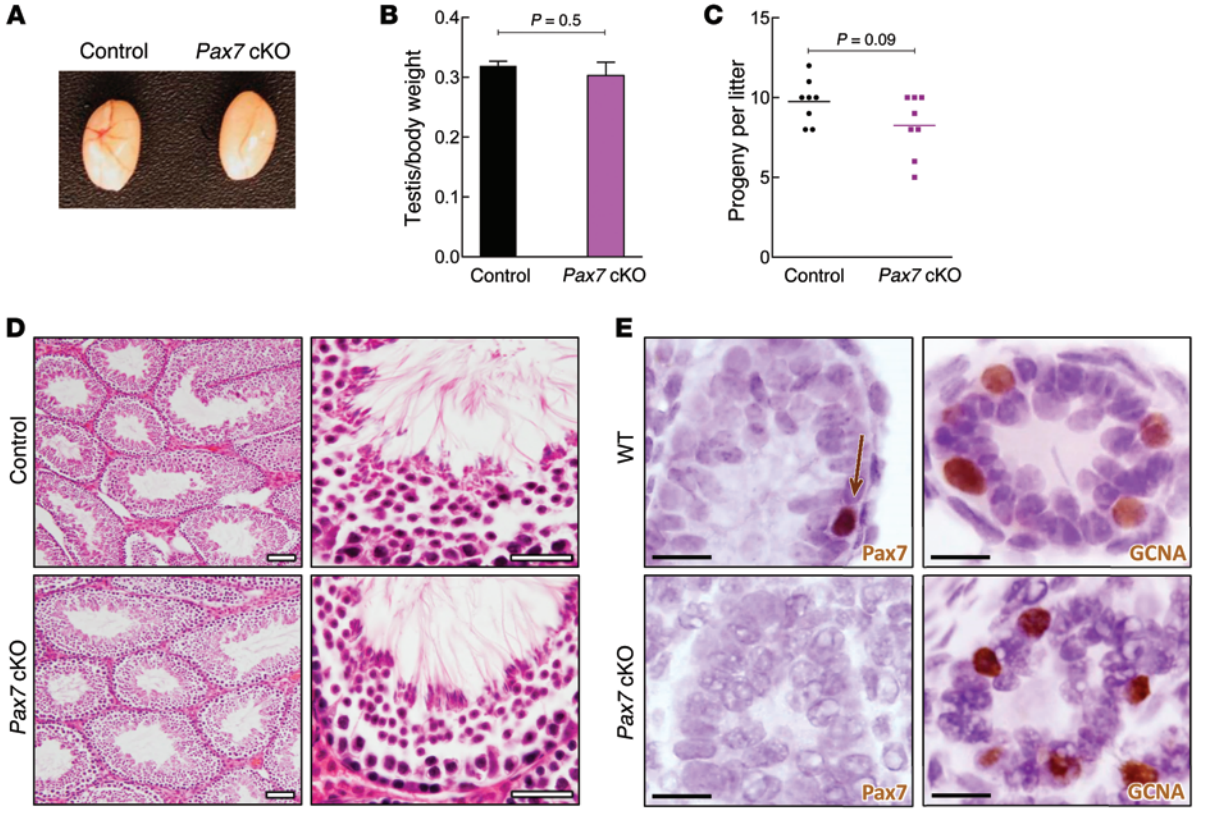

Figure 10. *Pax7* cKO in the male germline. For each analysis, n = 3 animals were evaluated per genotype. (**A**) Testes from floxed *Pax7*$^{fl/fl}$ control and *Pax7* cKO (*VC;Pax7*$^{-/fl}$) males at 6 months of age. No abnormalities or size differences were noted. (**B**) Testis weight expressed as percent of total body weight (6 months of age). (**C**) Fertility assays of 6 month-old males. Bars denote means. All floxed control and *Pax7* cKO males were fertile and sired litters of normal size. (**D**) Histological analyses at 6 months of age. No abnormalities in spermatogenesis or testis morphology were noted. (**E**) IHC analyses of *Pax7* cKO males at PD7. PAX7$^+$ spermatogonia were abundant and present in most tubules in wild-type controls (arrow), but absent in *Pax7* cKO tubules (multiple sections were stained and examined for each), confirming the specificity of the PAX7 antibody in testis sections. GCNA shows the presence of germ cells. Scale bars: 50 μm.

Here, we took advantage of lineage tracing as a method to explore the stem behavior of a novel population of spermatogonia defined by PAX7$^+$ expression. We propose some criteria by which stem cell lineage–tracing studies should be evaluated in the context of the adult testis, in the addition to the requirement for full-lineage maturation. First, we believe one important criterion is that the labeled germ cell clones begin as single cells. For example, lineage tracing initiated with a Cre driver expressed in broad subsets of spermatogonia (e.g., FOXO1$^+$ or PLZF$^+$ spermatogonia) would initiate labeling in A_{single}–A_{al16} spermatogonia, including larger chains of spermatogonia, only a few of which represent actual stem cells. Extending this logic to our present study, it is possible that only a subset of PAX7$^+$ spermatogonia function as stem cells, although the remarkable rarity of PAX7$^+$ spermatogonia is one argument against this possibility. Another criterion we believe should be considered is the long-term perdurance of labeled clones. Such perdurance excludes the possibility that the labeled cells represent transit-amplifying intermediates, which would be diluted out and thus disappear with time. In the lineage-tracing studies with the *mT/mG* reporter, we studied clones for up to 16 weeks (112 days) and observed no decrease in clone numbers, while the duration of spermatogenesis in mice is approximately 40 days (34).

Lack of genetic requirement for Pax7 in normal spermatogenesis in the mouse. In preliminary genetic studies, we did not find evidence for a functional requirement for *Pax7* in spermatogenesis. Germ cell–specific *Pax7* inactivation (confirmed by the apparent lack of PAX7 protein in germ cells) did not result in male infertility or have a discernible effect on spermatogenesis. It will be interesting to study the effect of *Pax7* inactivation in SSC cultures, which may exhibit phenotypes not apparent in vivo. Challenging these *Pax7* cKO mice with busulfan, however, demonstrated that lack of PAX7 delayed spermatogenic recovery, a finding that should be further explored, particularly as the number of animals analyzed was relatively small and busulfan was tested at only 1 concentration.

The lack of a functional requirement for fertility in the undisturbed testis — at least under laboratory conditions — may be surprising given the phylogenetic conservation of PAX7$^+$ spermatogonia. On the other hand, several other useful conserved and canonical stem cell markers, like Lgr5 (gut) and CD150 (hematopoiesis) are, also dispensable for stem cell function in the respective organs in which they serve (53–56). Although *Lgr5* conditional inactivation in intestinal epithelium yielded no apparent phenotype, simultaneous inactivation of *Lgr5* and *Lgr4* (which is expressed more broadly than *Lgr5*) enhanced an intestinal crypt loss phenotype observed with *Lgr4* (55). It is similarly possible

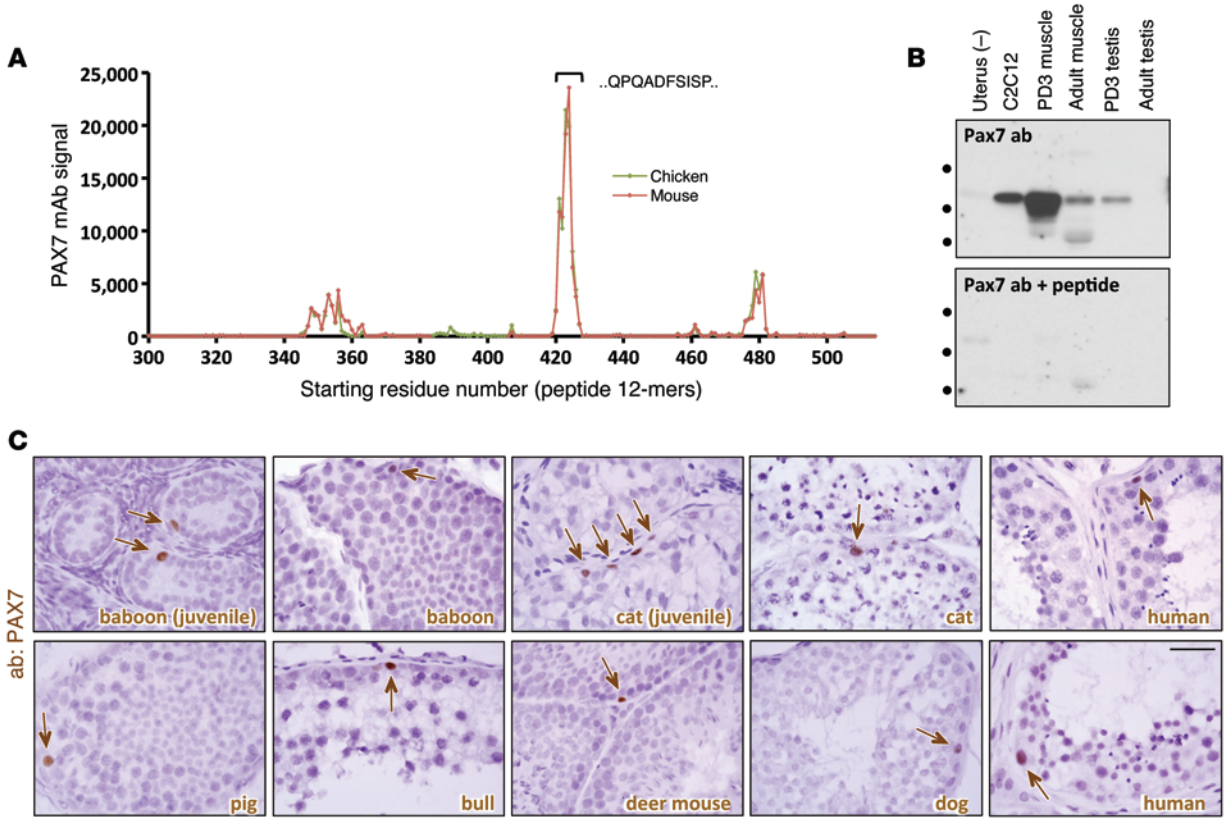

Figure 11. PAX7⁺ spermatogonia are conserved in mammals. (**A**) Epitope mapping of anti-PAX7 mouse monoclonal antibody (generated against chicken aa 320–523). Chicken and corresponding mouse polypeptide aa sequences were tiled as sequential 12-mers at 1-aa resolution. (**B**) PAX7 Western blot (uncropped to show all visible bands in lanes shown). Addition of blocking peptide (22 aa) confirmed that the anti-PAX7 monoclonal antibody bound to the QPQADFSISP epitope. C2C12, skeletal muscle myoblast cell line. Uterus was included as a negative control. Molecular weight markers denote 75, 50, and 37 kDa. (**C**) IHC of testes from 7 additional mammalian species, including juveniles for 2 species. PAX7⁺ spermatogonia (arrows) were rare and localized to the basement membrane. Scale bar: 25 μm.

that other factors — perhaps other *Pax* genes — are functionally redundant with *Pax7* and compensate for its loss, although we did not identify any *Pax* genes that were specifically expressed in SSCs in gene expression analyses. Furthermore, the floxed allele used for this study (*Pax7*$^{tm1.1Fan}$) was recently found to give rise to a hypomorphic mutation that expresses low levels of a truncated PAX7 protein from an alternative ATG start site, and thus does not appear to be a true biological or phenotypic null (32). In the more recently described floxed allele *Pax7*$^{tm1.1Thbr}$, the transcriptional start site and the first 3 exons are floxed, preventing the generation of any mRNA from the *Pax7* locus after Cre-mediated recombination (57). Thus, even though PAX7 protein was greatly reduced in the *Pax7* cKO analysis we performed with the *Pax7*$^{tm1.1Fan}$ allele (Figure 10E), it will be of interest to conduct future investigations with the *Pax7*$^{tm1.1Thbr}$ allele.

Implications for iatrogenic male infertility. Infertility is a common and well-known complication of cancer treatment that profoundly affects men and boys (41). Virtually all standard therapies (e.g., cytotoxic chemotherapies and radiotherapy) are highly toxic to the male germline. The likelihood of infertility with chemotherapy is drug-specific and dose-related. Alkylating agents pose the highest risk of infertility, with platinum analogs, anthracyclines, and nitrosoureas posing an intermediate level of risk (58). The germline is also very sensitive to radiation-induced damage. Doses of 1.2 Gy and higher are associated with an increased risk of infertility (58).

Remarkably, murine PAX7⁺ spermatogonia proved resistant to both radiotherapy and chemotherapy. They not only survived the immediate aftermath of these genotoxic insults, but also rapidly expanded, forming clusters of PAX7⁺ spermatogonia never observed in normal, untreated mice. Lineage-tracing studies confirmed that PAX7⁺ spermatogonia contribute to the restoration of spermatogenesis. Future studies will be needed to more fully define the extent of the role of PAX7⁺ spermatogonia as spermatogenic recovery cells and to determine the relative contributions to spermatogenic recovery of PAX7⁺ spermatogonia versus other spermatogonial subtypes. It is also interesting to consider the possibility that PAX7⁺ spermatogonia might contribute to the recovery of fertility in cancer patients, or that their failure to recover might account for permanent sterilization after chemotherapy or radiotherapy. If so, improved understanding of the biological pathways regulating the behavior of PAX7⁺ spermatogonia might someday lead to strategies to protect the male germline in cancer patients. It will also be interesting to explore the biological mechanisms that render PAX7⁺ spermatogonia resistant to genotoxic stresses.

The resistance of PAX7⁺ spermatogonia to both radiation and chemotherapy argues against models in which resistance is medi-

Table 1. The QPQADFSISP *PAX7* epitope is perfectly conserved in mammals, but not zebrafish or *Drosophila*

Species	Sequence
Gallus gallus (chicken)	407 SILSNPSGVPP**QPQADFSISP**LHGGLDTTNSI
Mus musculus (mouse)	386 SILSNPSAVPP**QPQADFSISP**LHGGLDSASSI
Rattus norvegicus (rat)	386 SILSNPSAVPP**QPQADFSISP**LHGGLDSASSI
Canis familiaris (dog)	519 SILSNPSAVPP**QPQADFSISP**LHGGLDSATSI
Felis catus (cat)	386 SILSNPSAVPP**QPQADFSISP**LHGGLDSATSI
Homo sapiens (human)	388 SILGNPSAVPP**QPQADFSISP**LHGGLDSATSI
Pan troglodytes (chimpanzee)	388 SILGNPSAVPP**QPQADFSISP**LHGGLDSATSI
Macaca mulatta (macaque)	388 SILSNPSAVPP**QPQADFSISP**LHGGLDSATSI
Papio anubis (baboon)	387 SILSNPSAVPP**QPQADFSISP**LHGGLDSATSI
Bos taurus (bull)	388 SILSNPSAVPP**QPQADFSISP**LHGGLDSATSI
Ornithorhynchus anatinus (platypus)	355 SILSNPSGVPP**QPQADFSISP**LHGGLDTTNSI
Danio rerio (zebrafish), *Pax7a*	389 SILSNPSAVPS**QPQH**D**FSISP**LHGGLEASNPI
Danio rerio (zebrafish), *Pax7b*	392 SILSNPSAVAP**QPQ**HE**FSISP**LHSSLEASNPI
Drosophila melanogaster (fruit fly), *gsb-n*	337 AQHGFPGGFA**QP**GHFG**S**QNYYHQDYSKLTID

ated by active drug efflux (MDR1 or other transporters), as is the case with several types of stem cells (e.g., the "side population" effect due to the efflux of fluorescent dyes) (59, 60).

In closing, PAX7$^+$ spermatogonia represent a rare but functionally important stem cell population in the healthy adult testis, and also serve an important role in spermatogenic recovery following injury to the germline, such as occurs after chemotherapy or radiotherapy. That PAX7$^+$ spermatogonia are rapidly cycling and yet resistant to such stress is a notable aspect of their biology.

Methods

mRNA analysis and PAX7 discovery. RNA preparation, microarray hybridization, normalization, quality control, and digital Northern analysis was performed as described previously (24). Additional data sets included in this analysis were intact PD2 testes and cultured SSCs established as previously described (61), both from FVB/n mice. The embryonic stem cell, embryonic gonad, and spermatogenic cell data sets were downloaded from GEO (accession nos. GSE4193, GSE4308, and GSE6916) (62–64). Probe sets were ranked based on signal strength in SSCs as a proportion of that in the intact adult testis.

Mouse strains and procedures. Mice harboring the *Pax7-Cre^{ERT2}* [B6;129-*Pax7$^{tm2.1(cre/ERT2)Fan}$*/J] and *Pax7^{fl}* [B6;129-*Pax7$^{tm1.1Fan}$*/J] alleles as well as the *R26R* [FVB.129S4(B6)-*Gt(ROSA)26Sor^{tm1Sor}*/J], *mT/mG* (tdTomato/eGFP) reporter [*Gt(ROSA)26Sor$^{tm4(ACTB-tdTomato,-EGFP)Luo}$*/J], and nuclear tdTomato reporter [B6.Cg-*Gt(ROSA)26Sor$^{tm9(CAG-tdTomato)Hze}$*/J] alleles were purchased from Jackson Laboratories (31–33, 35). Busulfan (CAS no. 55-98-1, TCI America) was dissolved in DMSO and administered as a single i.p. dose. EdU (catalog no. C10338, Invitrogen) was dissolved in water and injected i.p. (50 mg/kg). Cyclophosphamide was dissolved in PBS and administered at 150 mg/kg i.p. every 5 days for 25 days. Tamoxifen (catalog no. T5648, Sigma-Aldrich) was dissolved at 100 mg/ml in 100% ethanol, then resuspended at 20 mg/ml in corn oil. 2 mg tamoxifen was delivered i.p. to each adult mouse daily for 3 days. Neonatal mice (PD5 or earlier) were injected i.p. with 0.2 mg tamoxifen daily for 3 days. Whole-body irradiation was administered (single dose) while the mice were restrained in acrylic boxes at a dose rate of 1.44 Gy/min. No specific method for randomization for animal studies was used; investigators were not blinded.

Transplantation procedure. 2 testes from 1 *Pax7-Cre^{ERT2};tdTomato* (PD14) donor (mixed genetic background) were enzymatically digested with dispase (catalog no. 354235, BD) to obtain single cells that were resuspended in DMEM with 10% FBS plus 0.02% Trypan Blue (25). 5–10 μl of 9×10^3 cells/μl were transplanted by the efferent duct method into testes of 3 *Kit^W/Kit^{W-v}* mice (4–6 weeks old, mixed genetic background; stock no. 100410, Jackson Laboratories). Testis filling per blue dye was 50%–90% in each testis. To deplete T cells and promote engraftment, 50 μg anti-CD4 antigen (catalog no. MAB554, R&D Systems) was injected i.p. 3 times every other day starting on the day of transplantation. Testes were analyzed 4 weeks after transplantation.

Tissue processing, IHC, and immunofluorescence (IF). For IHC, tissues were fixed in 10% buffered formalin overnight, embedded in paraffin, and cut into 5-μm sections (except for the serial analysis of an entire testis and PAX7 cluster analyses, where 20-μm sections were used), with indirect detection performed as described previously (27).

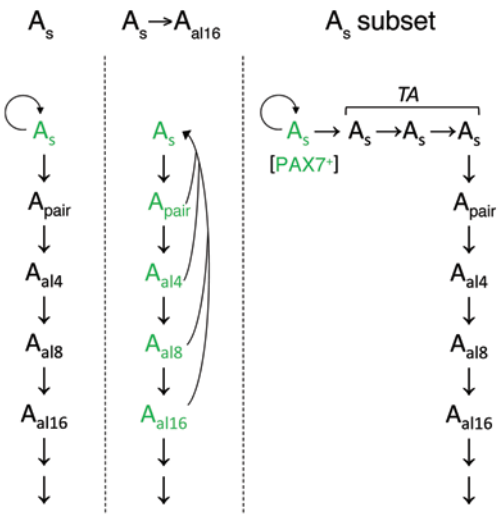

Figure 12. Models of stemness in mouse spermatogenesis. Spermatogonial subsets proposed as the bona fide stem cells are shown above each of the 3 models. In the classic A_{single} model (A_s), A_{single} spermatogonia are homogeneous and share stem cell identity (green), having the capacity for self-maintenance (circular arrows; refs. 3, 4, 66). More recently, models have been proposed arguing for greater plasticity among undifferentiated ($A_{single} \rightarrow A_{al16}$) spermatogonia, with chain fragmentation representing one possible mechanism by which stemness is maintained or regenerated (5). Although fragmentation has been shown to occur in vivo, its contributions to stem cell maintenance under normal conditions or after chemotherapy/radiation have not been formally established. Our findings that only a subset of A_{single} spermatogonia expressed PAX7 and that these spermatogonia functioned as stem cells suggests a new A_{single} subset model, whereby PAX7$^+$ spermatogonia are self-maintaining and may sit atop the hierarchy of spermatogenic differentiation. That A_{single} spermatogonia were heterogeneous and that only a subset functioned as stem cells was also suggested by previous studies (10, 67). If so, then this would suggest that some subset of A_{single} spermatogonia represent transit-amplifying (TA) intermediates. The number of such transit-amplifying steps between PAX7$^+$ A_{single} and A_{pair} spermatogonia is unknown. It will be interesting to determine whether ID4 and ERBB3, expressed in A_{single} spermatogonia, are expressed in overlapping or nonoverlapping subsets of spermatogonia relative to PAX7 (9, 49, 50). Other models are possible, such as ones combining different aspects of these models (i.e., fragmentation with the presence of PAX7$^+$ spermatogonia, if fragmentation is confirmed as a functionally significant biological process).

For whole-mount IF, seminiferous tubules were mechanically dissociated in PBS on ice and fixed overnight in 4% paraformaldehyde (PFA). Tubules were dehydrated in a series of methanol washes and stored at –20°C. To rehydrate and permeabilize, tubules were put through a series of washes with methanol and PBS plus 0.1% Tween-20, followed by incubation with 0.2% NP-40 for IF of nuclear proteins. Tubules were blocked in 2% BSA and PBS (catalog no. 37525, Thermo Scientific Blocker) for 2 hours, then in MOM block (catalog no. MKB-2213, Vector Labs), and primary antibody was added in 0.5% BSA and PBS with 0.02% sodium azide, followed by incubation at 4°C overnight. Tubules were washed 3 times for 10 minutes each in PBS at RT. Secondary antibody (Alexa Fluor 555 anti-rabbit, Alexa Fluor 488 anti-mouse, Alexa Fluor 555 anti-goat; catalog nos. A-21428, A-21121, and A-21432, respectively, Invitrogen) was added at 1:1,000 in 0.5% BSA and PBS for 2 hours at RT followed by DAPI staining (1:10,000 in PBS; catalog no. 46290, Pierce). Tubules were placed on glass slides and mounted in Vectashield (Vector Laboratories). For visualization of *mT/mG* clones in tissue sections, testes were embedded in OCT; sectioned; fixed for 30 minutes in 4% formalin, 7% picric acid, 20% and sucrose at 4°C; and then cryosectioned. Microscopy was performed with a Leica TCS SP5 confocal microscope.

Antibodies for IF and IHC. Antibodies and titers used were as follows: PAX7 (1:200 for IHC, 1:25 for IF; Developmental Studies Hybridoma Bank), FOXO1 (1:200 for IHC, 1:50 for IF; catalog no. 2880, Cell Signaling Technology), KIT (1:200 for IHC, 1:50 for IF; catalog no. 3074, Cell Signaling Technology), PLZF (1:10,000 for IHC; catalog no. AF2944, R&D Systems), caspase-3 (1:250 for IF; catalog no. 559565, BD Biosciences — Pharmingen), DSred (detects tdTomato; 1:100 for IF; catalog no. 632496, Clontech), GCNA (1:200 for IHC; provided by G.C. Enders, University of Kansas, Kansas City, Kansas, USA; ref. 39), RET (1:20 for IHC; catalog no. 18121, IBL America), GFRα1 (1:100 for IF; catalog no. AF560, R&D Systems).

X-gal staining. Whole-mount X-gal staining was performed by manually dissociating tubules, fixing in 4% PFA and PBS for 30 minutes at RT, and staining as previously described (43) for 6 hours to overnight, followed by refixing in 4% PFA and PBS overnight.

Epitope mapping and phylogenetic analyses. An arrayed microchip was designed by LC Sciences as described previously (65). The chip included 12-mer tiling peptides sequences with 1-aa resolution corresponding to the entire chicken polypeptide immunogen (aa 300–523; Genbank NP_990396.1). The corresponding mouse aa sequence was also arrayed on the same microchip, also at 1-aa resolution. Peptide sequences were acetyl-capped at the N terminus. PAX7 antibody (1 μg/ml) was hybridized to the microarray in 1× PBS 7.4 for 2 hours at 4°C, then washed in 1× PBS with 0.05% Tween-20 and 0.05% TritonX-100, pH 7.0. Detection was performed with an anti-mouse IgG/Alexa Fluor 647 conjugate (10 ng/ml) in binding buffer for 1 hour at 4°C. The array was scanned at 635 nm on an Axon GenePix 4000B Microarray Scanner. Sequences were obtained from NCBI (HomoloGene 55665 and accession nos. XP_003989659.1, XP_003891265.1, and XP_003428482.1) and manually aligned. Gonadal samples were described previously (45).

Western blotting. For the blocking experiment, a 22-residue blocking peptide PSAVPPQPQADFSISPLHGGLD, spanning the 10-aa epitope, was synthesized. The peptide (0.1 μg/μl) and antibody (20 ng/μl) were incubated at 4°C for 24 hours in 500 μl PBS, then centrifuged at 4°C for 15 minutes (11,525 *g*). The supernatants with and without blocking peptide (500 μl) were added to 2.5 ml 5% milk 1× TBST and applied to the Western blots.

Statistics. Statistics were calculated using GraphPad software. Error bars in all figures indicate SEM for at least 3 animals. For Fisher exact tests, 2-tailed comparisons were performed to calculate *P* values. A *P* value less than 0.05 was considered significant.

Study approval. This study was approved by the UT Southwestern Institutional Animal Care and Use Committee.

Acknowledgments

This work was supported by the David M. Crowley Foundation, NCI grants R01CA137181 and HD048690, and the State of Texas Norman Hackerman Advanced Research Program (010019-0060-2009). G.M. Aloisio was supported by a UT Southwestern Cecil H. and Ida Green Center for Reproductive Biological Sciences fellowship. The authors acknowledge the assistance of Kate Luby-Phelps and the UT Southwestern Live Cell Imaging Facility, a shared resource of the Harold C. Simmons Cancer Center, supported in part by NCI Cancer Center Support Grant P30CA142543. We thank Alexandra Ghaben, Rene Galindo, Lee Kraus, Andrew Zinn, Thomas Braun, Chen-Ming Fang, Michael Rudnicki, and Sean Morrison for helpful discussions.

Address correspondence to: Diego H. Castrillon, UT Southwestern Medical Center, Department of Pathology, NB6.452 6000 Harry Hines Boulevard, Dallas, Texas 75390-9072, USA. Phone: 214.648.4032; E-mail: diego.castrillon@utsouthwestern.edu.

1. Oatley JM, Brinster RL. Regulation of spermatogonial stem cell self-renewal in mammals. *Annu Rev Cell Dev Biol*. 2008;24:263–286.
2. de Rooij DG. Proliferation and differentiation of spermatogonial stem cells. *Reproduction*. 2001;121(3):347–354.
3. de Rooij DG, Russell LD. All you wanted to know about spermatogonia but were afraid to ask. *J Androl*. 2000;21(6):776–798.
4. Oakberg EF. Spermatogonial stem-cell renewal in the mouse. *Anat Rec*. 1971;169(3):515–531.
5. Nakagawa T, Sharma M, Nabeshima Y, Braun RE, Yoshida S. Functional hierarchy and reversibility within the murine spermatogenic stem cell compartment. *Science*. 2010;328(5974):62–67.
6. Jan SZ, Hamer G, Repping S, de Rooij DG, van Pelt AM, Vormer TL. Molecular control of rodent spermatogenesis. *Biochim Biophys Acta*. 2012;1822(12):1838–1850.
7. Yang QE, Oatley JM. Spermatogonial stem cell functions in physiological and pathological conditions. *Curr Top Dev Biol*. 2014;107:235–267.
8. Nagano MC, Yeh JR. The identity and fate decision control of spermatogonial stem cells: where is the point of no return? *Curr Top Dev Biol*. 2013;102:61–95.
9. Oatley MJ, Kaucher AV, Racicot KE, Oatley JM. Inhibitor of DNA binding 4 is expressed selectively by single spermatogonia in the male germline and regulates the self-renewal of spermatogonial stem cells in mice. *Biol Reprod*. 2011;85(2):347–356.
10. Nagano MC. Homing efficiency and proliferation kinetics of male germ line stem cells following transplantation in mice. *Biol Reprod*. 2003;69(2):701–707.
11. Brinster RL, Avarbock MR. Germline transmission of donor haplotype following spermatogonial transplantation. *Proc Natl Acad Sci U S A*. 1994;91(24):11303–11307.
12. Kanatsu-Shinohara M, Shinohara T. Spermatogonial stem cell self-renewal and development. *Annu Rev Cell Dev Biol*. 2013;29:163–187.
13. Kubota H, Avarbock MR, Brinster RL. Culture conditions and single growth factors affect fate determination of mouse spermatogonial stem cells. *Biol Reprod*. 2004;71(3):722–731.
14. Shinohara T, Avarbock MR, Brinster RL. Beta1-

and alpha6-integrin are surface markers on mouse spermatogonial stem cells. *Proc Natl Acad Sci U S A*. 1999;96(10):5504–5509.
15. Phillips BT, Gassei K, Orwig KE. Spermatogonial stem cell regulation and spermatogenesis. *Philos Trans R Soc Lond B Biol Sci*. 2010;365(1546):1663–1678.
16. Zhang Z, Shao S, Meistrich ML. The radiation-induced block in spermatogonial differentiation is due to damage to the somatic environment, not the germ cells. *J Cell Physiol*. 2007;211(1):149–158.
17. Yoshida S. Elucidating the identity and behavior of spermatogenic stem cells in the mouse testis. *Reproduction*. 2012;144(3):293–302.
18. McLean DJ. Spermatogonial stem cell transplantation and testicular function. *Cell Tissue Res*. 2005;322(1):21–31.
19. Brinster RL. Germline stem cell transplantation and transgenesis. *Science*. 2002;296(5576):2174–2176.
20. Kanatsu-Shinohara M, et al. Long-term proliferation in culture and germline transmission of mouse male germline stem cells. *Biol Reprod*. 2003;69(2):612–616.
21. Kanatsu-Shinohara M, Inoue K, Ogonuki N, Morimoto H, Ogura A, Shinohara T. Serum- and feeder-free culture of mouse germline stem cells. *Biol Reprod*. 2011;84(1):97–105.
22. Meng X, et al. Regulation of cell fate decision of undifferentiated spermatogonia by GDNF. *Science*. 2000;287(5457):1489–1493.
23. Relaix F, Zammit PS. Satellite cells are essential for skeletal muscle regeneration: the cell on the edge returns centre stage. *Development*. 2012;139(16):2845–2856.
24. Gallardo TD, et al. Genomewide discovery and classification of candidate ovarian fertility genes in the mouse. *Genetics*. 2007;177(1):179–194.
25. Yin H, Price F, Rudnicki MA. Satellite cells and the muscle stem cell niche. *Physiol Rev*. 2013;93(1):23–67.
26. Tanaka SS, et al. The mouse homolog of Drosophila Vasa is required for the development of male germ cells. *Genes Dev*. 2000;14(7):841–853.
27. Goertz MJ, Wu Z, Gallardo TD, Hamra FK, Castrillon DH. Foxo1 is required in mouse spermatogonial stem cells for their maintenance and the initiation of spermatogenesis. *J Clin Invest*. 2011;121(9):3456–3466.
28. Buaas FW, et al. Plzf is required in adult male germ cells for stem cell self-renewal. *Nat Genet*. 2004;36(6):647–652.
29. Naughton CK, Jain S, Strickland AM, Gupta A, Milbrandt J. Glial cell-line derived neurotrophic factor-mediated RET signaling regulates spermatogonial stem cell fate. *Biol Reprod*. 2006;74(2):314–321.
30. Vergouwen RP, Huiskamp R, Bas RJ, Roepers-Gajadien HL, Davids JA, de Rooij DG. Postnatal development of testicular cell populations in mice. *J Reprod Fertil*. 1993;99(2):479–485.
31. Lepper C, Fan CM. Inducible lineage tracing of Pax7-descendant cells reveals embryonic origin of adult satellite cells. *Genesis*. 2010;48(7):424–436.
32. Lepper C, Conway SJ, Fan CM. Adult satellite cells and embryonic muscle progenitors have distinct genetic requirements. *Nature*. 2009;460(7255):627–631.
33. Soriano P. Generalized lacZ expression with the ROSA26 Cre reporter strain. *Nat Genet*. 1999;21(1):70–71.
34. Franca LR, Avelar GF, Almeida FF. Spermatogenesis and sperm transit through the epididymis in mammals with emphasis on pigs. *Theriogenology*. 2005;63(2):300–318.
35. Muzumdar MD, Tasic B, Miyamichi K, Li L, Luo L. A global double-fluorescent Cre reporter mouse. *Genesis*. 2007;45(9):593–605.
36. Madisen L, et al. A robust and high-throughput Cre reporting and characterization system for the whole mouse brain. *Nat Neurosci*. 2010;13(1):133–140.
37. Bucci LR, Meistrich ML. Effects of busulfan on murine spermatogenesis: cytotoxicity, sterility, sperm abnormalities, and dominant lethal mutations. *Mutat Res*. 1987;176(2):259–268.
38. van Keulen CJ, de Rooij DG. Spermatogenetic clones developing from repopulating stem cells surviving a high dose of an alkylating agent. *Cell Tissue Kinet*. 1975;8(6):543–551.
39. Enders GC, May JJ. Developmentally regulated expression of a mouse germ cell nuclear antigen examined from embryonic day 11 to adult in male and female mice. *Dev Biol*. 1994;163(2):331–340.
40. Lu CC, Meistrich ML. Cytotoxic effects of chemotherapeutic drugs on mouse testis cells. *Cancer Res*. 1979;39(9):3575–3582.
41. Goldfarb S, Mulhall J, Nelson C, Kelvin J, Dickler M, Carter J. Sexual and reproductive health in cancer survivors. *Semin Oncol*. 2013;40(6):726–744.
42. Withers HR, Hunter N, Barkley HT Jr, Reid BO. Radiation survival and regeneration characteristics of spermatogenic stem cells of mouse testis. *Radiat Res*. 1974;57(1):88–103.
43. Gallardo T, Shirley L, John GB, Castrillon DH. Generation of a germ cell-specific mouse transgenic Cre line, Vasa-Cre. *Genesis*. 2007;45(6):413–417.
44. Castrillon DH, et al. Toward a molecular genetic analysis of spermatogenesis in Drosophila melanogaster: characterization of male-sterile mutants generated by single P element mutagenesis. *Genetics*. 1993;135(2):489–505.
45. Tarnawa ED, Baker MD, Aloisio GM, Carr BR, Castrillon DH. Gonadal expression of foxo1, but not foxo3, is conserved in diverse mammalian species. *Biol Reprod*. 2013;88(4):103.
46. Roosen-Runge EC. Comparative aspects of spermatogenesis. *Biol Reprod*. 1969;1:24–31.
47. Fuller MT. Genetic control of cell proliferation and differentiation in Drosophila spermatogenesis. *Semin Cell Dev Biol*. 1998;9(4):433–444.
48. Kawakami A, Kimura-Kawakami M, Nomura T, Fujisawa H. Distributions of PAX6 and PAX7 proteins suggest their involvement in both early and late phases of chick brain development. *Mech Dev*. 1997;66(1–2):119–130.
49. Abid SN, et al. A-single spermatogonia heterogeneity and cell cycles synchronize with rat seminiferous epithelium stages VIII-IX. *Biol Reprod*. 2014;90(2):32.
50. Chan F, et al. Functional and molecular features of the Id4+ germline stem cell population in mouse testes. *Genes Dev*. 2014;28(12):1351–1362.
51. Snippert HJ, Clevers H. Tracking adult stem cells. *EMBO Rep*. 2011;12(2):113–122.
52. Rojas-Ríos P, González-Reyes A. Concise review: The plasticity of stem cell niches: a general property behind tissue homeostasis and repair. *Stem Cells*. 2014;32(4):852–859.
53. Barker N, et al. Identification of stem cells in small intestine and colon by marker gene Lgr5. *Nature*. 2007;449(7165):1003–1007.
54. Kiel MJ, Yilmaz OH, Iwashita T, Yilmaz OH, Terhorst C, Morrison SJ. SLAM family receptors distinguish hematopoietic stem and progenitor cells and reveal endothelial niches for stem cells. *Cell*. 2005;121(7):1109–1121.
55. de Lau W, et al. Lgr5 homologues associate with Wnt receptors and mediate R-spondin signalling. *Nature*. 2011;476(7360):293–297.
56. Wang N, et al. The cell surface receptor SLAM controls T cell and macrophage functions. *J Exp Med*. 2004;199(9):1255–1264.
57. Gunther S, Kim J, Kostin S, Lepper C, Fan CM, Braun T. Myf5-positive satellite cells contribute to Pax7-dependent long-term maintenance of adult muscle stem cells. *Cell stem cell*. 2013;13(5):590–601.
58. Howell SJ, Shalet SM. Spermatogenesis after cancer treatment: damage and recovery. *J Natl Cancer Inst Monogr*. 2005;(34):12–17.
59. Drach J, Zhao S, Drach D, Korbling M, Engel H, Andreeff M. Expression of MDR1 by normal bone marrow cells and its implication for leukemic hematopoiesis. *Leuk Lymphoma*. 1995;16(5–6):419–424.
60. Petriz J. Flow cytometry of the side population (SP). *Curr Protoc Cytom*. 2013; Chapter 9:Unit9.23.
61. Falciatori I, Lillard-Wetherell K, Wu Z, Hamra FK, Garbers DL. Deriving mouse spermatogonial stem cell lines. *Methods Mol Biol*. 2008;450:181–192.
62. Kurimoto K, et al. An improved single-cell cDNA amplification method for efficient high-density oligonucleotide microarray analysis. *Nucleic Acids Res*. 2006;34(5):e42.
63. Small CL, Shima JE, Uzumcu M, Skinner MK, Griswold MD. Profiling gene expression during the differentiation and development of the murine embryonic gonad. *Biol Reprod*. 2005;72(2):492–501.
64. Namekawa SH, et al. Postmeiotic sex chromatin in the male germline of mice. *Curr Biol*. 2006;16(7):660–667.
65. Pellois JP, Zhou X, Srivannavit O, Zhou T, Gulari E, Gao X. Individually addressable parallel peptide synthesis on microchips. *Nat Biotechnol*. 2002;20(9):922–926.
66. Huckins C. Cell cycle properties of differentiating spermatogonia in adult Sprague-Dawley rats. *Cell Tissue Kinet*. 1971;4(2):139–154.
67. Suzuki H, Sada A, Yoshida S, Saga Y. The heterogeneity of spermatogonia is revealed by their topology and expression of marker proteins including the germ cell-specific proteins Nanos2 and Nanos3. *Dev Biol*. 2009;336(2):222–231.